Disentangling Ripple Effect from Systemic Risk in Stock Market Dynamics: The Case of Silicon Valley Bank Run *†

Kanji Suzuki[a,b‡], Yuji Sakurai[c], Keiichi Goshima[d§]

[a]ETH Zurich, Switzerland

[b]University of Zurich, Switzerland

[c]International Monetary Fund, United States

[c]Yokohama National University, Japan

May 25, 2024

Abstract

We develop a new model named the Common Auto-Regressive Jump Intensity Score-driven with Triggering probability (CARJIST) model. It captures the unobservable systemic risk and the ripple effect by applying the Generalized Autoregressive Score (GAS) framework. The unobservable systemic risk is modeled as a common jump with the time-varying intensity. The ripple effect is modeled as the time-varying probability of triggering the realization of common jumps. The model allows us to decompose the realization of systemic risk in multiple stock returns into the systemic risk and ripple effect components. We apply the model for the 2023 U.S. regional banking crisis. Our main findings are as follows: First, the systemic risk of the regional banks interacts with the large commercial banks, but the ripple effect does not. Second, we find that the Federal Funds rate and term spread impact the systemic risk and ripple effect of both regional banks and large commercial banks. Our estimate indicates the 1% increase in the Federal Funds rate leads to around 3.5% increase in the probability of common jumps among those regional banks. Third, we document that the systemic risk of the regional banks is affected by the aggregate deposit outflow whereas the ripple effect is influenced by the option-implied risk appetite of the stock investors. Finally, we find that the CoVaR-based linkage of the regional banks strengthened after the SVB collapse.

*The authors deeply appreciate...

†The views expressed in this study are those of the authors and do not necessarily reflect the positions of institutions. Especially, the views expressed herein are those of the authors and should not be attributed to the IMF, its Executive Board or its management.

‡Corresponding author. E-mail address: kanji.suzuki.0321@gmail.com

§Goshima greatly acknowledges the financial support of JSPS KAKENHI Grant Number JP21K13329 and Nomura School of Advanced Management.

Keywords: Non-normality, Contagion, Financial Stability,
Banking Crisis, Dynamic Conditional Score models

JEL Classification Numbers: G01, G21, C58.

1 Introduction

The collapse of the Silicon Valley Bank (SVB) in March of 2023 forced investors and regulators to re-assess the systemic risk of the U.S. banking sector, especially of regional banks. It is argued that rising interest rates caused mark-to-market valuation losses on securities held by the SVB and other regional banks. When such unrealized losses exceed uninsured deposits, depositors of these banks become concerned about the risk and withdraw their deposits (Choi et al. (2023)). [1] However, how U.S. banking sector stock prices have evolved before and during the SVB collapse is not yet well studied. A key challenge is to model stock price crashes occurring on different dates.

In this paper, we address this challenge by developing a new time series model. We ask the following two research questions: How is the systemic risk of U.S. regional banks realized, and (2) whether systemic risk is associated with macroeconomic variables or driven by market risk appetite? To do so, we develop a new model named the "Common Auto-Regressive Jump Intensity Score-driven with Triggering probability model" (CARJIST). The model allows us to decompose the stock price crashes of U.S. banks into two components: latent systemic risk component and the ripple effect component. First, the latent systemic risk is modeled as a common jump intensity following Das and Uppal (2004). We apply the Generalized Autoregressive Score paradigm proposed by Creal et al. (2013) so that the common jump intensity is time-varying based on its score. The second component is the probability of triggering the realization of the common jump. We allow the probability to be time-varying based on its score under the GAS framework similar to the common jump intensity. We consider that the triggering probability measures the ripple effect because the stock price crash of one bank increases the possibility of another bank's stock price crash when the triggering probability is higher.

The CARJIST model has two advantages. First, we can capture stock price jumps that occur at different times, but we can still track the commonality of jumps. This is important because the stock price crashes or failures of U.S. regional banks did not occur on the same day. Second, it allows us to extract the time-varying systemic risk and ripple effect easily.

We estimate the model for stock returns for two sets of banks from January 1, 2017, to December 31, 2023. The first group consists of five regional banks: First Foundation Inc. (FFWM), First Republic Bank (FRCB), SVB Financial Group (SVB), Signature Bank (SBNY) and Western Alliance Bancorporation (WAL). These five regional banks were selected based on the low cumulative excess return during the SVB panic, as documented by Choi et al. (2023). The second group comprises

[1] There are studies providing a comprehensive overview of SVB failure such as Metrick (2024) and Acharya et al. (2023).

five large commercial banks. It consists of Bank of America Corporation (BAC), Citigroup Inc. (CITI), JP Morgan (JPM), U.S. Bancorp (USB) and Wells Fargo & Company (WFC) based on the total asset size. Our main research interest is U.S. regional banks. For comparison purposes, we estimate the CARJIST model for large commercial banks.

As a preliminary analysis, we calculate the skewness of five regional banks and five commercial banks by rolling with a window size of sixty. Figure 1 illustrates the first principal component of skewness for both the regional and commercial banks. The gray dotted line represents Mar 8, 2023, when the first collapse of the SVB occurred. The principal component of regional banks sharply climbs up on that day and remains at a high level thereafter. The principal component of commercial banks experiences a modest increase around the SVB run, settles and starts to rise again in early June. The correlation between these two principal components before SVB collapse is 0.0420, and in the post-collapse period, it is 0.516. This result leads us to the hypothesis that the extreme events in regional banks spread to commercial banks.

We estimate the model based on the maximum likelihood estimation. Specifically, we estimate the EGARCH parameters for each bank's stock return as a first step and then common-jump-related parameters for all banks. As model outputs, we obtain a time series of the common jump intensity and triggering probability after the estimation. We study whether the common jump intensity and triggering probability are impacted by or forecast macro-financial variables by running VAR (1) models.

Our main findings are as follows: First, we document that both the common jump intensity and triggering probability increased dramatically on the day after the SVB failure. It is noteworthy that our estimates of the time-varying intensity and probability at time t are based solely on the data available up to time t, therefore, they are not influenced by future data beyond time t, which are not accessible to investors in making decisions.

Second, our VAR results show that the common jump intensity of the regional banks interacts with that of the large commercial banks. In other words, the systemic risks of the regional banks and the large commercial banks tend to amplify each other. However, we do not find a similar pattern for the ripple effect described by the triggering probability. The triggering probability of the regional banks does not interact with one of the large commercial banks.

Third, we investigate whether the systemic risk and ripple effect are associated with macroeconomic fundamentals and/or financial market stress. Three observations were made in this study. (1) The common jump intensity and triggering probability of both banking groups are influenced by Federal Funds rates and the term spread. Our estimates for the regional bank model indicate a 1% increase in the Federal Funds rate leads to a 0.3% increase in the common jump intensity and a 1.2% increase in the triggering probability. This is equivalent to a 3.55% increase in the probability of the common jump among regional banks. (2) The common jump intensity of the regional banks is impacted by the aggregate flow of deposits in the U.S. banking sector. (3) The triggering probability of the regional banks is impacted by the CBOE SKEW index, which represents the downside risk of the stock market.

These results suggest that the systemic risk of the regional banks, measured by the common jump intensity, reflects the fundamental fragility of the financial system. By contrast, the ripple effect measured by the triggering probability reflects the investor's risk appetite.

We also compute the CoVaR, which is widely used as a systemic risk measure. We document that the co-movements between CoVaR for regional banks have become stronger during the SVB failure period than during the pre-SVB failure period. Moreover, our result shows that the tail-dependency between commercial banks and SVB boosts after the crisis.

As a robustness check, we employ different model specifications and test whether the main results change. Specifically, we employ a different scaling function for the dynamics of the common jump intensity and triggering probability under the GAS framework. Overall, our main results qualitatively remain the same.

Our study belongs to the emerging literature on SVB failure analysis. Most of these studies are based on the event study or panel data analysis. In contrast to these studies, we employ a sophisticated time series model to analyze the stock market crash when SVB failed.

The remainder of this paper is organized as follows. Section 2 reviews the literature. The proposed model is described in Section 3. Section 4 describes the data. Section 5 presents the empirical results. Section 6 concludes.

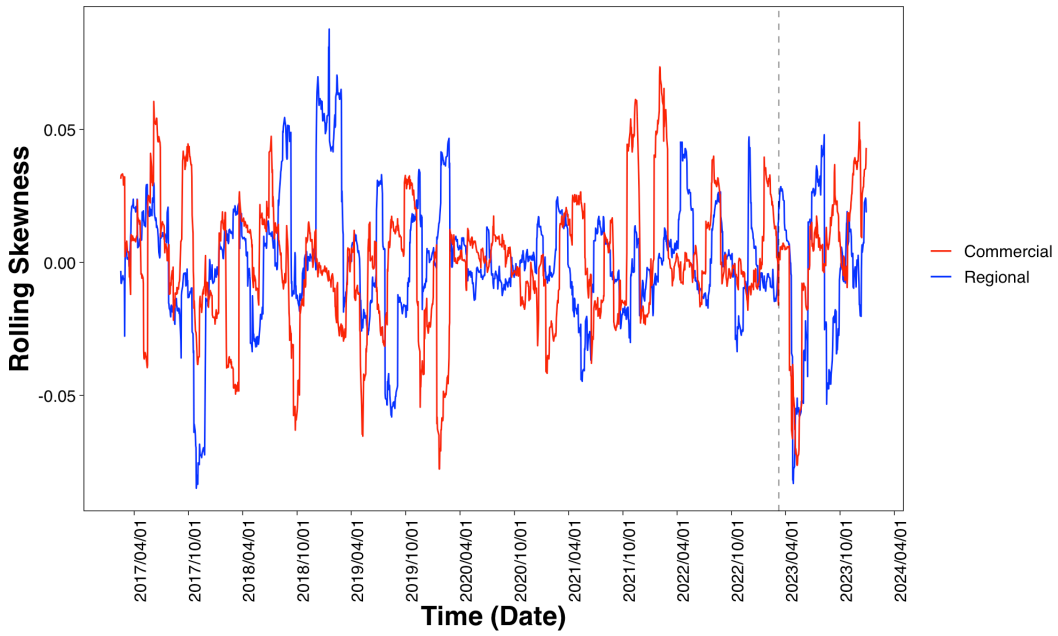

Figure 1: First principal component of the rolling skewness for both regional banks and commercial banks with a window size of thirty. The dotted line represents the value on Mar 9, 2023.

2 Literature Review

This paper contributes to three strands of the literature.

The first strand is empirical studies of SVB failure. Yousaf and Goodell (2023) study the reactions of equity market sectors to the SVB run by calculating the abnormal returns of eleven U.S. equity sectors. They observe that the financial sector has the most significant negative impact. Choi et al. (2023) investigate the factors contributing to spillovers during the SVB run by regressing the cumulative excess return on bank-level characteristics. They find that uninsured deposits and unrealized losses in held-to-maturity are associated with negative excess returns. Additionally, they emphasize the significant stress experienced by mid-sized regional banks whereas very large banks exhibit superior performance. Jiang et al. (2023) construct an economic framework to illustrate how rapid monetary tightening devalues bank assets, triggers withdrawals of uninsured deposits, and ultimately leads to solvency bank runs. Their event study validates that SVB has the highest proportion of uninsured deposits in assets. Our study further strengthens these findings by offering quantitative assessments of systemic risk and ripple effects through the lens of a sophisticated time-series model. These insights are invaluable for understanding the mechanisms underlying the SVB failure.

The second strand is the literature on the parametric modeling of the common jump process. Ballestra et al. (2023) adapts the conditional jump model using the GAS framework, resulting in a nonlinear shock term in the dynamics of the conditional jump intensity. Li and Maheu (2020) proposes a multivariate GARCH-jump mixture model in which the jump component is determined by a combination of correlated multivariate normal shocks and a multinomial random variable that indicates the occurrence of jumps. Das and Uppal (2004) develop a system of multivariate jump-diffusion processes wherein the number of jumps is uniform across all assets. Aït-Sahalia et al. (2015) develop a multivariate Hawkes process in which the intensity of jumps exihibits cross-excitation as well as self-excitation. The primary difference in the CARJIST model is the introduction of a novel variable: the triggering probability. This variable effectively evolves individual jumps into common jumps with a few parameters, whereas ensuring alignment in the direction of jump sizes across assets.

The third strand is the modeling of systemic risks and risk management. Tobias and Brunnermeier (2016) proposes a measure of systemic risk named CoVaR. The change in CoVaR conditioned on another institution experiencing distress relative to its median state is valuable for assessing institutions' exposure to the distress of individual institutions, as well as for analyzing the directional network among institutions. Brownlees et al. (2020) utilize quantile regression and conduct backtesting of CoVaR for U.S. financial institutions spanning the period from 1866 to 1933. They substantiated that CoVaR effectively explains the patterns of individual bank deposit declines observed during panic periods. Girardi and Ergün (2013) examines the systemic risk contributions of four financial industry groups in the U.S. during the pre-financial crisis period of 2008. They employ the DCC model with student-t error terms and find a significant increase in the CoVaRs of all financial industry groups before the crisis. By contrast, we employ the CARJIST model to estimate

the CoVaR. This model, featuring the inclusion of common jumps, is well-suited for capturing tail co-movement.

3 Methodology

3.1 Model

We propose a new model named Common Auto-Regressive Jump Intensity Score-driven with Triggering probability (CARJIST) to describe how a jump in a certain asset increases the probability of the jump in itself and other assets. In this model, the innovation of the volatility-filtered return of a certain asset is decomposed into a smooth term and a common jump term. The common jump term has a common discrete component across assets, modeling the arrivals of unusual news that affects asset prices.

Let $\mathbf{r}_t = (r_{1,t}, \cdots, r_{N,t})$ be the vector of returns of N assets at time t. The information set at time t is defined as $\mathcal{F}_t = \{r_{i,\tau} \text{ for } \forall i = 1, \cdots, N \text{ and } \tau = 1, \cdots, t\}$. Given the information set $\mathcal{F}_{t-1}$, we assume that $r_{i,t}$ is written as

$$r_{i,t} = \mu_i + \sigma_{i,t}\epsilon_{i,t} \tag{3.1}$$

for all $i = 1, \cdots, N$, where $\sigma_{i,t}$ is the mean-reverting level of the volatility of i given $\mathcal{F}_{t-1}$, $\epsilon_{i,t}$ is the volatility-filtered return with unconditional variance one, and μ_i is the unconditional mean of $r_{i,t}$.

Denote as $\boldsymbol{\epsilon}_t$ the vector of volatility-filtered returns. We employ the EGARCH(1,1) model to filter-out the return
footnote

$$\log(\sigma_{i,t+1}) - \log(\bar{\sigma}_i) = \alpha_i(\log(\sigma_{i,t}) - \log(\bar{\sigma}_i)) + \beta_i(|\epsilon_{i,t}| - \sqrt{\frac{2}{\pi}}) \tag{3.2}$$

for all $i = 1, \cdots, N$, where $\bar{\sigma}_i$ is the mean-reverting level of $\sigma_{i,t}$. α_i is the auto-coefficient and β_i is the volatility of volatility..

The EGARCH(1,1)-filtered return is modeled as

$$\epsilon_{i,t} = z_{i,t} + b_{i,t}e_{i,t} \tag{3.3}$$

for all $i = 1, \cdots, N$, where $b_{i,t}$ is an indicator variable that determines the realization of the jump innovation $e_{i,t}$. $\mathbf{z}_t = (z_{1,t}, \cdots, z_{N,t})^T$ follows multivariate normal distribution with mean $\mathbf{0}$ and variance Σ. The conditional distribution of $b_{i,t}$ given $\mathcal{F}_{t-1}$ is a Bernoulli distribution with the conditional triggering probability p_t.

$$p(b_{i,t} = g_i|\mathcal{F}_{t-1}) = \begin{cases} p_t & \text{when} \quad b_{i,t} = 1, \\ 1 - p_t & \text{when} \quad b_{i,t} = 0 \end{cases} \tag{3.4}$$

for $i = 1, 2, \cdots, N$. The independence of $b_{i,t}$ across i and t is assumed. The jump innovations $e_{1,t}, \cdots, e_{N,t}$ have the following common components:

$$e_{i,t} = \sum_{k=1}^{n_t}(\delta_i Z_{k,t} + \theta_i) - \lambda_t\theta_i \tag{3.5}$$

for all $i = 1, \cdots, N$, where $Z_{k,t}$ is the common jump randomness governed by the standard normal distribution independent across k and t. θ_i and δ_i control the mean and variance of the jump when it realizes for asset i. [2] Then, $Z_{k,t}$ determines the direction and the absolute size of the common jump, and δ_i determines the heterogeneous relative size around the mean. n_t is the number of common jump arrivals at time t. The conditional distribution of n_t given $\mathcal{F}_{t-1}$ is a Poisson distribution with the conditional jump intensity λ_t.

$$p(n_t = j|\lambda_t) = \frac{e^{-\lambda_t}\lambda_t^j}{j!}, j = 0, 1, 2, \cdots. \tag{3.6}$$

We subtract $\lambda_t\theta_i$ on the right-hand side of 3.5 to guarantee that the unconditional expectation of $e_{i,t}$ is zero. The independence between $z_{i,t}$, $b_{i,t}$, n_t and $Z_{k,t}$ is assumed. In a later analysis, we set θ_i as a constant across i and denote it as θ for simplicity.

Note that n_t and $Z_{k,t}$ for $k = 1, \cdots, n_t$ are common across i in contrast to $b_{i,t}$. Given that $p_t = E(b_{i,t}|\mathcal{F}_{t-1})$ holds from 3.4, the jump innovation $e_{i,t}$ is realized with an average probability of p_t, independently across assets. When p_t is small, $e_{i,t}$ is more likely to manifest as individual jumps because $b_{i,t}$ cuts off the realization. Conversely, when p_t is large, $e_{i,t}$ transforms into common jumps, as p_t allows it to realize across multiple assets. In this regard, we view p_t as representing the ripple effect within the market, underscoring its role in transmitting jump innovations derived from $Z_{k,t}$ across assets. Moreover, equation 3.6 gives $\lambda_t = E(n_t|\mathcal{F}_{t-1})$. We regard that λ_t as characterizing the latent systemic risk within the market, signifying its role in gauging the potential likelihood of jumps across all assets. By combining p_t and λ_t, the CARJIST model allows us to capture the characteristics of tail comovements in multiple assets.

To construct the joint probability of $\boldsymbol{\epsilon}_t$ given $\mathbf{r}_t$, we start with the conditional joint probability given the number of jumps and its realization for each asset. Denote the information set at time t as $\mathcal{F}_t$. Let $\boldsymbol{\delta} = (\delta_1, \cdots, \delta_N)^T$, $\mathbf{g} = (g_i, \cdots, g_N)^T$ and $\mathbf{b}_t = (b_{1,t}, \cdots, b_{N,t})^T$. Considering $n_t = j$ and $b_{i,t} = g_i$ for $i = 1, \cdots, N$, the conditional joint distribution is a multivariate normal distribution.

$$\begin{aligned} &f(\boldsymbol{\epsilon}_t|\mathcal{F}_{t-1}, n_t = j, \mathbf{b}_t = \mathbf{g}) = \\ &\quad \frac{1}{(2\pi)^{N/2}|\Sigma_{t,j,\mathbf{g}}|^{1/2}} \exp\left(-\frac{1}{2}(\boldsymbol{\epsilon}_t - \boldsymbol{\theta}_{t,j,\mathbf{g}})^T\Sigma_{t,j,\mathbf{g}}^{-1}(\boldsymbol{\epsilon}_t - \boldsymbol{\theta}_{t,j,\mathbf{g}})\right) \end{aligned} \tag{3.7}$$

where

$$\begin{aligned} \boldsymbol{\theta}_{t,j,\mathbf{g}} &= (\theta g_1(j - \lambda_t), \cdots, \theta g_N(j - \lambda_t))^T, \\ \Sigma_{t,j,\mathbf{g}} &= \Sigma + ((\boldsymbol{\delta}\boldsymbol{\delta}^T) \circ (\mathbf{g}\mathbf{g}^T))j. \end{aligned}$$

[2] The jump-size term $Z_{k,t}$ is common across assets. This formulation ensures that the jump realizes the same signs across assets with a small number of parameters. For instance, if we consider a common jump model that posits different jump-size terms for each asset, additional parameters such as correlations between jumps or asymmetries are requisite to guarantee that the sizes of common jumps are correlated across assets.

Let $\mathcal{G}_N = \{(g_1, \cdots, g_N) | g_1 \in (0,1), \cdots, g_N \in (0,1)\}$. Using the equation 3.7, the joint distribution of $\boldsymbol{\epsilon}_t$ is written as

$$f(\boldsymbol{\epsilon}_t | \mathcal{F}_{t-1}) = \sum_{j=0}^{\infty} \sum_{\mathbf{g} \in \mathcal{G}_N} f_{t,j,\mathbf{g}} \tag{3.8}$$

where

$$f_{t,j,\mathbf{g}} = f(\boldsymbol{\epsilon_t} | \mathcal{F}_{t-1}, n_t = j, \mathbf{b}_t = \mathbf{g}) p(n_t = j | \mathcal{F}_{t-1}) p(b_{1,t} = g_1 | \mathcal{F}_{t-1}) \cdots p(b_{N,t} = g_N | \mathcal{F}_{t-1}). \tag{3.9}$$

In practice, we truncate the sum by a finite number n_{max}. Then, the conditional likelihood of $\boldsymbol{\epsilon}_t$ given $\mathcal{F}_{t-1}$ entails the summation of $n_{max} \times 2^N$-terms. [3]

We vary the market-risk parameters λ_t and p_t using the GAS framework proposed by Creal et al. (2013). The GAS framework enables the integration of time-varying parameters into conventional parametric models by leveraging the score of the log-likelihood function. Following Ballestra et al. (2023), we make $\phi_t = \log(\lambda_t)$ time-varying instead of λ_t itself to avoid λ_t becoming negative. The first derivative of the conditional log-likelihood given $\mathcal{F}_{t-1}$ with regard to ϕ_t is written in closed form.

$$\frac{\partial f(\boldsymbol{\epsilon}_t | \mathcal{F}_{t-1})}{\partial \phi_t} = \sum_{j=0}^{\infty} \sum_{\mathbf{g} \in \mathcal{G}_N} \frac{f_{t,j,\mathbf{g}}}{f(\boldsymbol{\epsilon}_t | \mathcal{F}_{t-1})} \nabla^{\phi}_{t,j,\mathbf{g}} \tag{3.10}$$

where

$$\nabla^{\phi}_{t,j,\mathbf{g}} = \frac{\partial \log f_{t,j,\mathbf{g}}}{\partial \phi_t} = j - \lambda_t - \theta \lambda_t \mathbf{g}^T \Sigma^{-1}_{t,j,\mathbf{g}} (\boldsymbol{\epsilon}_t - \boldsymbol{\theta}_{t,j,\mathbf{g}}). \tag{3.11}$$

We introduce scaling in equation 3.10 using a method similar to that used by Ballestra et al. (2023). Specifically, we scale $\nabla^{\phi}_{t,j,\mathbf{g}}$ using conditional variance and define a driving force of ϕ_t. The derivation of this formula is presented in Appendix A.1.

$$\tilde{s}^{\phi}_t = \frac{E(n_t | \mathcal{F}_t) - \lambda_t}{\sqrt{\lambda_t + \theta^2 \lambda_t^2 E(\mathbf{g}^T \Sigma^{-1}_{t,j,\mathbf{g}} \mathbf{g} | \mathcal{F}_{t-1})}} - \sum_{j=0}^{\infty} \sum_{\mathbf{g} \in \mathcal{G}_N} \frac{f_{t,j,\mathbf{g}}}{f(\boldsymbol{\epsilon}_t | \mathcal{F}_{t-1})} \frac{\theta \lambda_t \mathbf{g}^T \Sigma^{-1}_{t,j,\mathbf{g}} (\boldsymbol{\epsilon}_t - \boldsymbol{\theta}_{t,j,\mathbf{g}})}{\sqrt{\lambda_t + \theta^2 \lambda_t^2 E(\mathbf{g}^T \Sigma^{-1}_{t,j,\mathbf{g}} \mathbf{g} | \mathcal{F}_{t-1})}}. \tag{3.12}$$

In the empirical part, the scaling variance is calculated using a numerical computation. If we ignore the scaling in 3.12, $\tilde{s}^{\phi}_t$ is the difference between the ex-post and ex-ante count of common jumps, which is similar to the shock term in Maheu and McCurdy (2004), with an adjusting term derived from the score of $\log f(\boldsymbol{\epsilon_t} | \mathcal{F}_{t-1}, n_t = j, \mathbf{b}_t = \mathbf{g})$.

Next, we consider to vary p_t in the GAS framework. We take the logit of p_t to guarantee that p_t is in $[0,1]$. By differentiating the log-likelihood by $l_t = \text{logit}(p_t)$, we obtain

$$\frac{\partial f(\boldsymbol{\epsilon}_t | \mathcal{F}_{t-1})}{\partial l_t} = \sum_{j=0}^{\infty} \sum_{\mathbf{g} \in \mathcal{G}_N} \frac{f_{t,j,\mathbf{g}}}{f(\boldsymbol{\epsilon}_t | \mathcal{F}_{t-1})} \nabla^{\phi}_{t,j,\mathbf{g}} \tag{3.13}$$

[3] If we consider the common jump model that assumes an independent number of jumps across assets as in Aït-Sahalia et al. (2015), the computation of the likelihood requires a sum of n^N_{max}-terms. Therefore, our CARJIST model demonstrates greater parsimony than this type of model, yet it retains the capability to describe observations found in the actual data.

where

$$\nabla^{l}_{t,j,\mathbf{g}} = \frac{\partial \log f_{t,j,\mathbf{g}}}{\partial l_t} = \sum_{i=1}^{N} g_i - N p_t. \tag{3.14}$$

Using this, the driving force of l_t is defined as

$$\tilde{s}^{l}_{t} = \frac{\sum_{i=1}^{N} E(g_i|\mathcal{F}_t) - N p_t}{\sqrt{N p_t (1-p_t)}}. \tag{3.15}$$

If we ignore the scaling in 3.15, $\tilde{s}^{l}_{t}$ is the difference between the sum of the ex-post and ex-ante counts of common jump realizations. In this case, $\tilde{s}^{l}_{t}$ increases when jumps are inferred to be realized in multiple assets ex-post.

Using 3.12 and 3.15, the time-varying structures of ϕ_t and l_t are formulated as:

$$\begin{pmatrix} \phi_{t+1} - \bar{\phi} \\ l_{t+1} - \bar{l} \end{pmatrix} = \begin{pmatrix} a_\phi & 0 \\ 0 & a_l \end{pmatrix} \begin{pmatrix} \phi_t - \bar{\phi} \\ l_t - \bar{l} \end{pmatrix} + \begin{pmatrix} b_\phi & b_{\phi,l} \\ b_{l,\phi} & b_l \end{pmatrix} \begin{pmatrix} \tilde{s}^{\phi}_{t} \\ \tilde{s}^{l}_{t} \end{pmatrix} \tag{3.16}$$

where $\bar{\phi}$ is the unconditional mean of ϕ_t, and $\bar{l}$ is the unconditional mean of l_t. In this formulation, a_ϕ is the autoregressive parameter of ϕ_t, indicating its self-persistence over time, and b_ϕ denotes the sensitivity of λ to the driving force. Analogously, (a_l, b_l) is the counterpart of (a_ϕ, b_ϕ) that determines the time-varying structure of l_t. $b_{\phi,l}$ and $b_{l,\phi}$ allows the interaction between ϕ_t and p_t, which describes the successive occurrence of common jumps induced by certain assets. Since the derivative of ∇^{ϕ}_{t} with regards to l_t is zero, it is justifiable to scale the driving forces of ϕ_t and l_t separately.

3.2 Estimation Procedure

We estimate the CARJIST model in three steps. First, the EGARCH(1,1) model is estimated using the quasi-maximum likelihood estimation. We filter the conditional volatility out in each time series based on the EGARCH estimates and denote the filtered returns as $\tilde{\boldsymbol{\epsilon}} = (\tilde{\epsilon}_{1,t}, \cdots, \tilde{\epsilon}_{N,t})^T$. Hereafter, we maximize the log-likelihood:

$$l(\boldsymbol{\theta}) = \sum_{t=1}^{T} \log f(\tilde{\boldsymbol{\epsilon}}_t | \mathcal{F}_{t-1}) \tag{3.17}$$

where $\boldsymbol{\theta}$ is the set of parameters involved in the modeling of volatility-filtered returns $\boldsymbol{\epsilon}_t$.

Second, we assume that λ_t and p_t are invariant and estimate $(\bar{\lambda}, \bar{p})$ along with $\boldsymbol{\delta}$. In this process, the covariance matrix Σ of the normal shock $\mathbf{z}_t$ is endogenously determined so that the sample covariance matrix is equivalent to the analytical

unconditional variance and covariance given as [4]

$$E(\epsilon_{i,t}^2) = \Sigma_{ii} + \bar{p}\bar{\lambda}(\delta_i^2 + \theta^2), \tag{3.18}$$

$$\mathrm{Cov}(\epsilon_{i,t}, \epsilon_{t,j}) = \Sigma_{ij} + \bar{p}^2\bar{\lambda}(\delta_i\delta_j + \theta^2). \tag{3.19}$$

Third, the GAS parameters $(a_\phi, b_\phi, a_l, b_l, b_{\phi,l}, b_{l,\phi})$ are estimated whiwhereas the estimates in step 2 are plugged into log-likelihood 3.17. In this procedure, $\bar{\phi}$ and $\bar{l}$ are estimated as $\log(\bar{\lambda})$ and $\mathrm{logit}(\bar{p})$, respectively. [5]

3.3 Identifiability: Separating the Ripple Effect from the Systemic Risk?

The identifiability of λ_t and p_t is discussed. Figure 2 plots the news impact on (a) $\tilde{s}_t^\phi$ and (b) $\tilde{s}_t^l$ for the two-dimensional CARJIST model. The x-axis represents $\epsilon_{1,t}$, and the y-axis represents $\epsilon_{2,t}$. Both $\tilde{s}_t^\phi$ and $\tilde{s}_t^l$ ncrease when the two returns take high values in the same direction. The noteworthy difference is that $\tilde{s}_t^\phi$ increase when the two returns take the opposite signs, whereas $\tilde{s}_t^l$ is low. This is attributed to the CARJIST model treating this scenario as an outcome of a correlated normal shock along with a jump in a single asset.

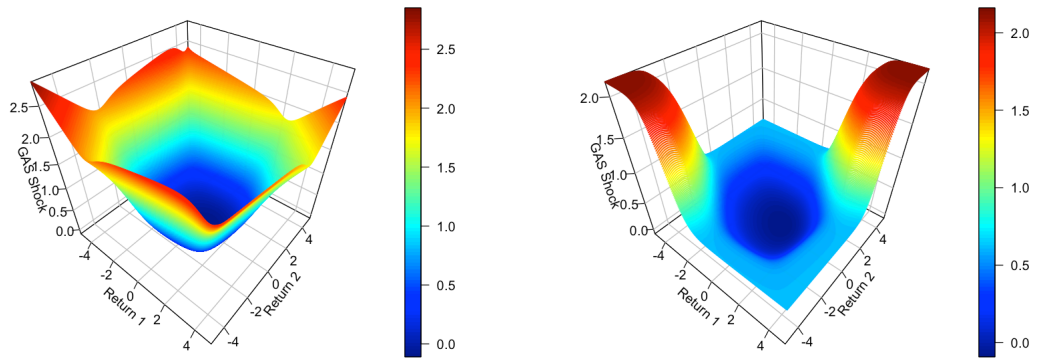

(a) (b)

Figure 2: News impact on (a) $\tilde{s}_t^\phi$ and (b) $\tilde{s}_t^l$ for the two-dimensional CARJIST where $\delta_1 = \delta_1 = 1, \theta = 0.3, \lambda_t = 0.5, p_t = 0.3, \Sigma_{11} = 0.95, \Sigma_{22} = 0.95$ and $\Sigma_{12} = \Sigma_{21} = 0.1$. The x-axis and the y-axis represents the EGARCH-filtered return of the asset 1 and of the asset 2, respectively.

[4]The analytical unconditional variance and covariance given in equation 3.18 and 3.19 are only true when λ_t and p_t are constants, that is when $\lambda_t = \bar{\lambda}$ and $p_t = \bar{p}$. When these two variables are time-varying, the computation of the unconditional variance and covariance becomes difficult owing to the correlation between them. In the second step of the estimation procedure, we assume that λ_t and p_t are constants, thereby justifying the use of equation 3.18 and 3.19.

[5]This calculation is based on approximations $\bar{\phi} = E[\log(\lambda_t)] \approx \log(E[\lambda_t)] = \log(\bar{\lambda})$ and $\bar{l} = E[\mathrm{logit}(p_t)] \approx \mathrm{logit}(E[p_t]) = \mathrm{logit}(\bar{p})$.

We obtain closed-form expressions for the mean, variance, skewness and kurtosis of returns $r_{i,t}$.

$$
\begin{aligned}
E(r_{i,t}|\mathcal{F}_{t-1}) &= \mu_i, && (3.20)\\
\mathrm{Var}(r_{i,t}|\mathcal{F}_{t-1}) &= \sigma^2_{i,t}(\Sigma_{ii} + p_t\lambda_t(\delta_i^2 + \theta^2)), && (3.21)\\
\mathrm{Skew}(r_{i,t}|\mathcal{F}_{t-1}) &= \frac{p_t\lambda_t\theta(3\delta_i^2 + \theta^2)}{(\Sigma_{ii} + p_t\lambda_t(\delta_i^2 + \theta^2))^{\frac{3}{2}}}, && (3.22)\\
\mathrm{Kurt}(r_{i,t}|\mathcal{F}_{t-1}) &= 3 + \frac{p_t\lambda_t(3\delta_i^4 + 6\delta_i^2\theta^2 + \theta^4)}{(\Sigma_{ii} + p_t\lambda_t(\delta_i^2 + \theta^2))^2} && (3.23)
\end{aligned}
$$

where Σ_{ii} is the (i,i)-th element of Σ. Equation 3.21 implies that conditional volatility can be written as a product of the GARCH volatility and the volatility associated with $\epsilon_{i,t}$. It follows that the common component $\lambda_t p_t$ drives the conditional volatility of each asset. This common component leads to volatility clustering across assets and encapsulates how bad news can escalate volatility throughout the market. Similarly, equation 3.22 and 3.23 demonstrate that skewness and kurtosis incorporate the common component $\lambda_t p_t$, highlighting our model's adaptability in capturing co-movements that manifest in the higher moments of returns.

Furthermore, our CARJIST model incorporates a dynamic correlation through λ_t and p_t. The conditional correlation between $r_{i,t}$ and $r_{j,t}$ is

$$
\mathrm{Corr}(r_{i,t}, r_{j,t}|\mathcal{F}_{t-1}) = \frac{\Sigma_{ij} + p_t^2\lambda_t(\delta_i\delta_j + \theta^2)}{\sqrt{(\Sigma_{ii} + p_t\lambda_t(\delta_i^2 + \theta^2))(\Sigma_{jj} + p_t\lambda_t(\delta_j^2 + \theta^2))}} \tag{3.24}
$$

where Σ_{ij} is the (i,j)-th element of Σ. Regarding the common jump variables, the numerator has the term $p_t^2\lambda_t$ whereas the denominator has the term $p_t\lambda_t$. It follows that the change in p_t affects the correlation when the $p_t\lambda_t$ is constant in contrast to the marginal moments. The intuitive understanding is that the change in p_t increases the correlation in the first order, whereas the change in λ_t does not affect the correlation. In this sense, p_t controls the extent of co-movements, and λ_t controls the potential risk in the market. Note that EGARCH volatility disappears in the conditional correlation in our specification.

4 Data

We obtained historical data comprising the closing prices of five regional banks: First Foundation Inc. (FFWM), First Republic Bank (FRCB), SVB Financial Group (SVB), Signature Bank (SBNY), and Western Alliance Bancorporation (WAL). These banks are selected based on their demonstrated low cumulative excess returns during SVB collapse, as documented by Choi et al. (2023). For commercial banks, we focus on the top five institutions based on consolidated assets as of December 2023. These institutions include the Bank of America Corporation (BAC), Citigroup Inc. (CITI), JP Morgan (JPM), U.S. Bancorp (USB) and Wells Fargo & Company (WFC). The sampling period spans from January 1, 2017, to December

31, 2023, encompassing the regional bank crisis starting on March 9, 2023. To estimate the model parameters, we calculate the daily arithmetic return for each bank. All data are available from Refinitiv Eikon.

Table 1 summarizes the descriptive statistics for the daily returns of the five regional banks. We have 1760 observations for FFWM and WAL, whereas SVB, SBNY and FRCB have missing records due to market halting. SVB data is unavailable from March 10 to March 27, 2023. SBNY data is unavailable from March 13 to March 27, 2023. FRCB is unavailable from May 1 to May 2, 2023. The minimum values observed for SVB, SBNY and FRCB are nearly minus one, reflecting a substantial loss in market value in Mar 2023. High levels of maximum values and skewness are also recorded because of the harsh oscillations after the crisis. Moreover, all the regional banks have high kurtosis levels. This observation highlights the strong fat-tail property of returns, which motivates us to use the jump model.

	FFWM	FRCB	SVB	SBNY	WAL
Obs.	1760	1758	1748	1749	1760
Mean	0.0002	0.0002	0.0048	0.0089	0.0008
Min	-0.331	-0.905	-0.996	-0.998	-0.471
Max	0.224	1.703	3.000	4.484	0.492
Std. Dev.	0.030	0.098	0.147	0.171	0.036
Skewness	0.020	6.544	9.220	13.086	-0.178
Kurtosis	16.60	121.82	150.67	296.77	49.39

Table 1: Descriptive statistics of daily arithmetic returns of five U.S. regional banks. SVB, SBNY and FRCB have missing records due to the market halting. Missing values are removed to calculate the statistics.

Table 2 reports the descriptive statistics of five commercial banks. There are no missing observations in the sample period. All banks are fat-tailed in comparison to the normal distribution.

	BAC	CITI	JPM	USB	WF
Obs.	1760	1760	1760	1760	1760
Mean	0.0005	0.0002	0.0006	0.0001	0.0002
Min	-0.154	-0.193	-0.150	-0.144	-0.159
Max	0.178	0.180	0.180	0.174	0.145
Std. Dev.	0.021	0.022	0.018	0.020	0.021
Skewness	0.369	0.048	0.377	0.142	-0.016
Kurtosis	11.01	13.52	14.41	10.23	7.95

Table 2: Descriptive statistics of daily arithmetic returns of five U.S. commercial banks.

We conduct Jarque-Bera (JB) and Kolmogorov-Smirnov (KS) tests to examine whether a univariate normal distribution can explain the time series of regional and commercial banks. For all banks, the hypothesis of normality is strongly rejected with the 1 % statistical significance. Furthermore, we also test the multivariate

normality of the joint distribution of five regional banks using the methods of Mardia (1970), rejecting the normality regarding both skewness and kurtosis with the 1 % statistical significance. Multivariate normality is also strongly rejected for the joint distribution of commercial banks. These results suggest that an alternative model is needed to describe non-normality in the joint distribution of banks.

5 Results

5.1 Model Estimation

Following the procedure described in section 3.2, we estimate the model for regional and commercial banks, separately. The maximum number of jumps is truncated by a finite number $n_{max} = 50$ in accordance with Ballestra et al. (2023). [6]

Our dataset includes missing observations attributed to the market halting of the SVB, SBNY and FRCB. In the estimation process, when confronted with missing observations in the dataset at a given time, we adopt an approach wherein the model is considered as if it were designed for a smaller dimension, accommodating the available information while accounting for the absence of certain data points. [7]

Table 3 shows the parameter estimates of EGARCH(1,1) model for the five regional banks. The sample standard deviation is used as an estimator of $\bar{\sigma}_i$. We observe the high persistence of conditional volatility for all stocks, which describes the existence of volatility clustering.

Table 3: Parameter estimates of EGARCH(1,1) model for five regional banks. First Foundation Inc. (FFWM), First Republic Bank (FRCB), SVB Financial Group (SVB), Signature Bank (SBNY), and Western Alliance Bancorporation (WAL) are investigated.

	FFWM	FRCB	SVB	SBNY	WAL
μ	0.0013^{***}	0.0012^{***}	0.0028^{***}	0.0009^{***}	0.0011^{***}
α	0.96^{***}	0.99^{***}	0.99^{***}	0.98^{***}	0.96^{***}
β	0.17^{***}	0.17^{***}	0.13^{***}	0.31^{***}	0.16^{***}

* Denote significance level at the 10 % level.
** Denote significance level at the 5 % level.
*** Denote significance level at the 1 % level.

Table 4 provides parameter estimates of the CARJIST model for the five regional banks. Based on the values of δ_i, the comparative magnitude of the common jumps is greatest in SVB, followed by SBNY and FRCB. This observation aligns

[6] This value is sufficiently large, as Ballestra et al. (2023) notes that the likelihood of experiencing over 50 jumps is virtually negligible (3.62e-20) when the jump intensity stands at ten.

[7] Blasques et al. (2021) proposes an unbiased simulation-based estimator for data with missing observations. However, our CARJIST model emphasizes the tail and thus requires a large simulation suze. Thus, we employ a simple approach that ignores the missing observations.

with expectations considering that these three banks experienced bankruptcy. The mean θ of the common jump size has a positive value, indicating the presence of jump-induced fluctuations both downward and upward. The persistence parameter a_ϕ takes a value close to one, which shows the successive occurrences of jumps, and the responsive parameter b_ϕ demonstrates that the intensity varies across time. Moreover, the substantial value of a_l implies a strong persistence in the degree of comovements among regional banks. The positivity of b_l shows that market resilience is lost because of the simultaneous crash of regional banks. The level of $b_{\phi,l}$ highlights that the infrequent large move in an individual bank weakens the resilience of all the investigated regional banks.

Table 4: Parameter estimates of the CARJIST model for five regional banks. First Foundation Inc. (FFWM), First Republic Bank (FRCB), SVB Financial Group (SVB), Signature Bank (SBNY), and Western Alliance Bancorporation (WAL) are investigated.

δ_{FFWM}	1.287^{***}
δ_{FRCB}	1.971^{***}
δ_{SVB}	2.461^{***}
δ_{SBNY}	2.005^{***}
δ_{WAL}	1.319^{***}
θ	0.195^{***}
$\bar{\phi}$	-0.395^{***}
$\bar{l}$	-1.86^{***}
a_ϕ	0.991^{***}
b_ϕ	0.159^{***}
a_l	0.859^{***}
b_l	0.438^{***}
$b_{\phi,l}$	0.265
$b_{l,\phi}$	0.050^{***}

* Denote significance level at the 10 % level.
** Denote significance level at the 5 % level.
*** Denote significance level at the 1 % level.

Using the estimated model, we extract the common jump intensity λ_t and triggering probability p_t. Figure 3a displays the dynamics of λ_t. We observe that the intensity sharply increases on March 10, 2023, which is adapted for the record on March 9, 2023. SVB failure strongly intensifies the jump intensity and thus escalates systemic risks in the regional bank market. Furthermore, the Figure shows that the intensity persists at a high level following the bank run. Figure 3b depicts the dynamics of p_t. Similar to λ_t, p_t exhibits an increase on March 10, 2023. Furthermore, on the same day, the returns of all banks except for SVB plummeted by

over -50%, rendering the SVB untradable. The crash precipitated a pronounced tail co-movement among the five stocks in subsequent trading days. The fluctuating triggering probability after the crisis destroys the resilience of these regional banks. These findings are consistent with the scenario of a contagion effect triggered by deposit outflows initially prompted by concerns about SVB's financial vulnerability, as described by Acharya et al. (2023). Note that both the model variables remain silent from March 2020 to September 2020. This is because the EGARCH component effectively absorbs volatility, as shown in Figure 4.

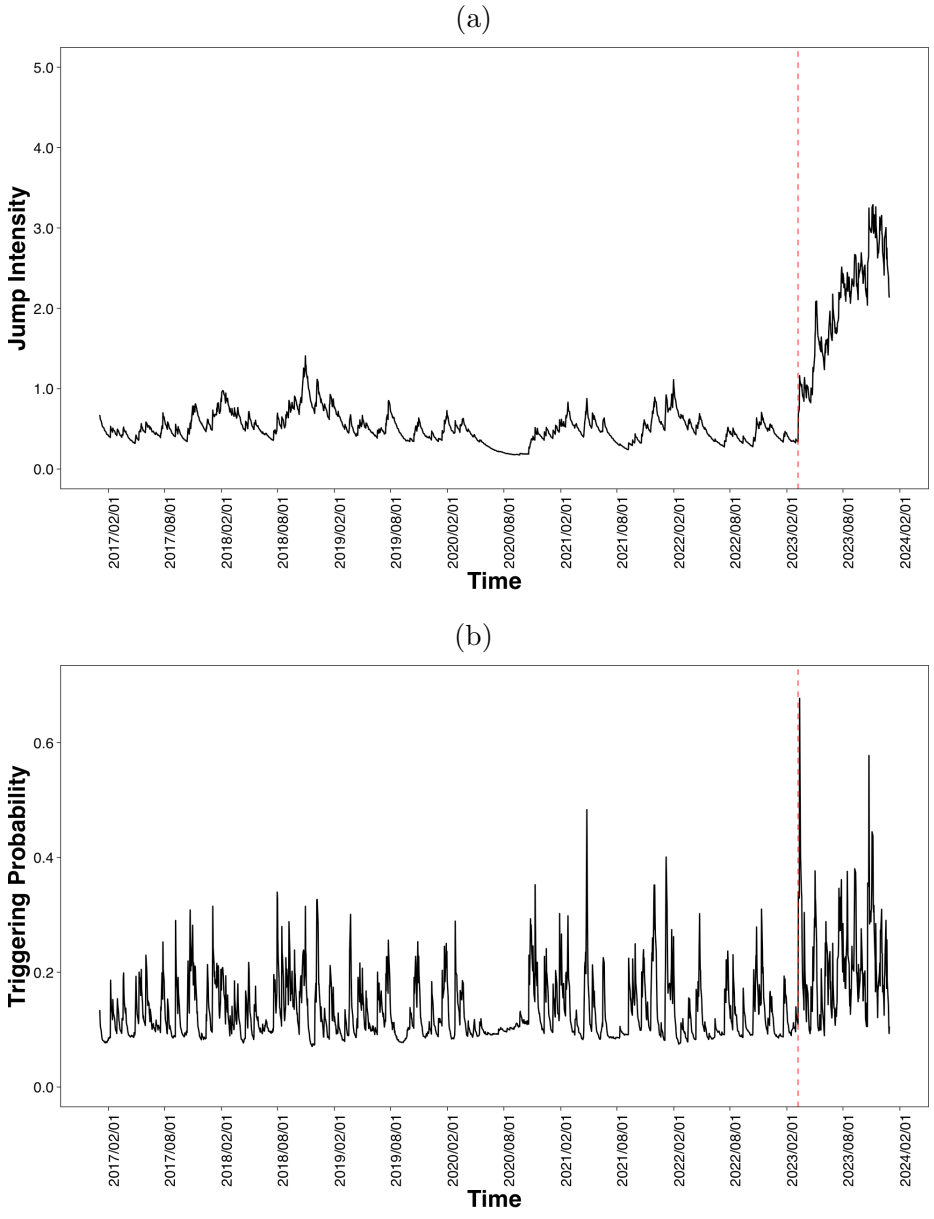

Figure 3: (a) jump intensity and (b) triggering probability of five regional banks extracted from the CARJIST model. The red point represents the value on Mar 9, 2023.

Figure 4 shows the time-varying conditional volatilities of the five regional banks.

Given equation 3.21, conditional volatility results from the product of the EGARCH component $\sigma_{i,t}$ and the jump component linked to $\epsilon_{i,t}$. The blue line is the conditional volatility, and the black line is the EGARCH component. As the unconditional expectation of the jump component is one, the difference between the two lines describes the adjustment of EGARCH volatility due to the jump component. In particular, conditional volatility gains sharply around Mar 9, 2023, simultaneously for all the regional banks. This is the implication emerging from the common component $\lambda_t p_t$ in equation 3.18. Additionally, there is a negligible disparity between the black and blue lines throughout the COVID-19 period, indicating a lesser impact of the jump components in explaining volatility during this period.

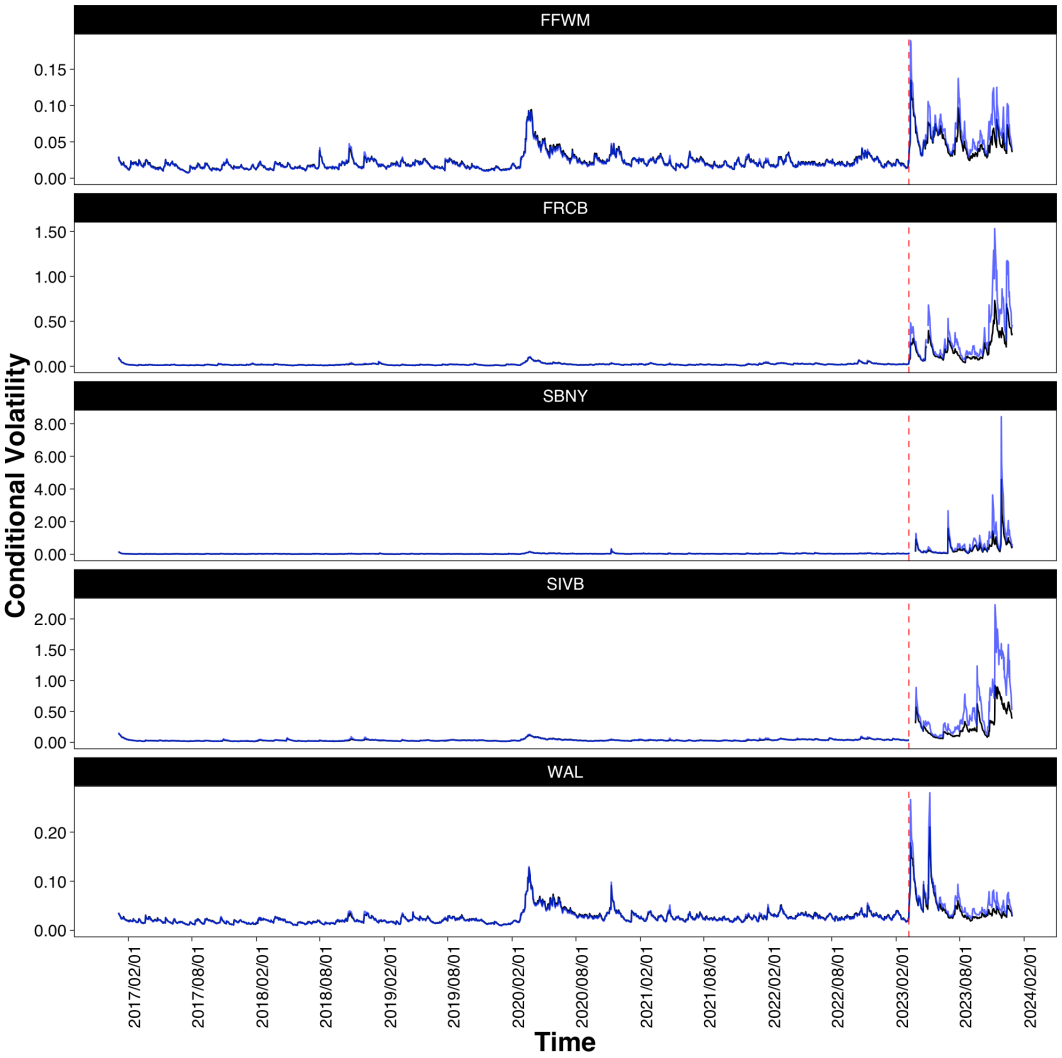

Figure 4: The time-varying conditional volatility of five regional banks from the CARJIST model. The blue line is the conditional volatility, and the black line is the EGARCH component. The red line represents Mar 9, 2023. First Foundation Inc. (FFWM), First Republic Bank (FRCB), SVB Financial Group (SVB), Signature Bank (SBNY), and Western Alliance Bancorporation (WAL) are investigated.

Figure 5 provides the (a) ex-ante and (b) ex-post probabilities of common jumps. We recognize that a common jump occurs at time t if $n_t \geq 1$ and $g_{i,t} = 1$ for more than three assets. This analysis is crucial for evaluating the existence and attributes of common jumps, thus enriching our understanding of the intricate interconnectivity inherent to asset dynamics. In Figure 5a, we observe a sharp hike after the SVB shortcoming on Mar 9, 2023, due to the increase of both λ_t and p_t. This shows the adaptive property of our CARJIST model, which modifies the model variables to improve the fitting. In Figure 5b, several common jumps are inferred to occur around Mar 9, 2023. Notably, the ex-post common jumps are still observed until November 2023. This is because these regional banks suffer significant losses in market value, resulting in highly volatile stock prices.

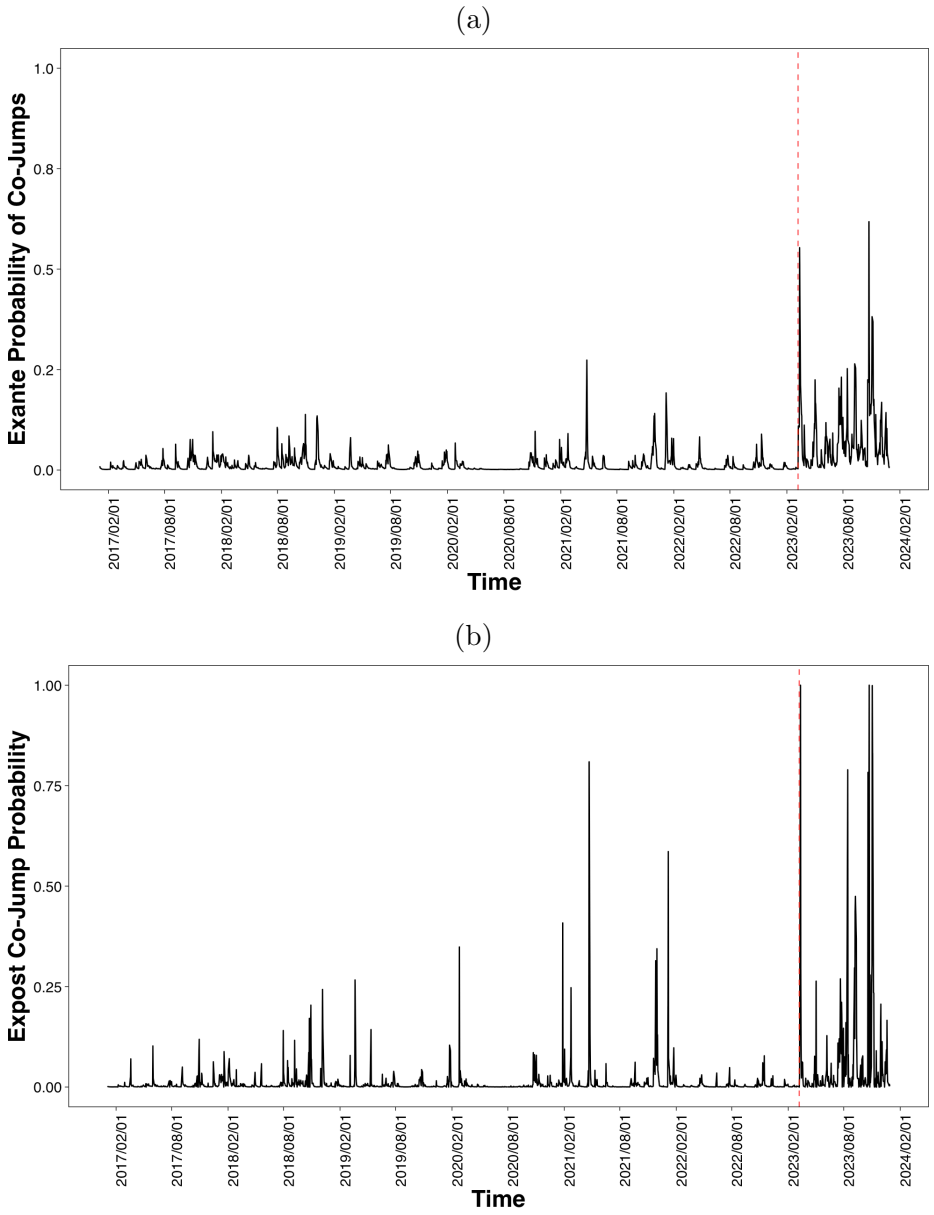

Figure 5: The (a) ex-ante and (b) ex-post probability that multiple jumps occur concurrently across more than three regional banks. The red point represents the value on Mar 9, 2023.

Figure 6 illustrates the estimated jump size volatility parameter δ_i plotted against the uninsured deposit rate of regional banks reported in Q4 of 2022. [8] We observe a positive relationship between these variables. A high level of the jump volatility parameter suggests an increased likelihood of extreme events occurring in the return time series. Hence, Figure 6 reinforces the argument that reliance on uninsured deposits may exacerbate financial fragility because of the possibility of rapid withdrawals, as highlighted in various studies (e.g., Acharya et al. (2023), Choi et al.

[8]The data of the uninsured deposit rates are available at the BankSuite tool provided by FDIC; https://banks.data.fdic.gov/bankfind-suite.

(2023), Jiang et al. (2023)).

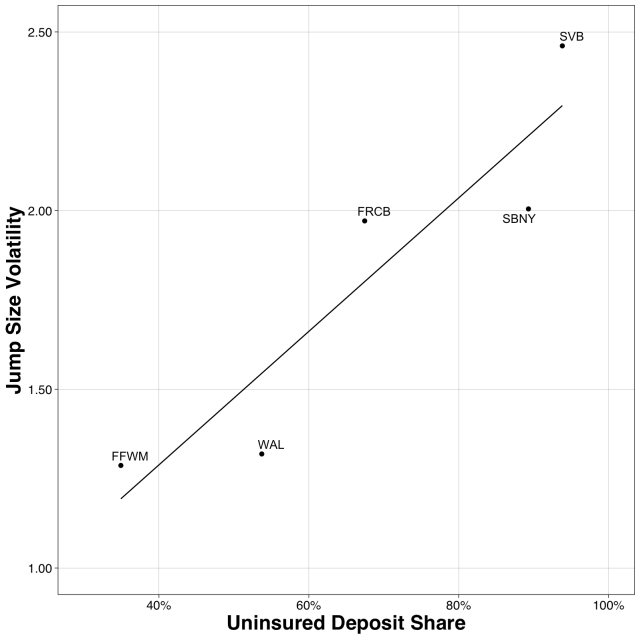

Figure 6: Plot of the estimated jump size volatility against the uninsured deposit rate of regional banks. First Foundation Inc. (FFWM), First Republic Bank (FRCB), SVB Financial Group (SVB), Signature Bank (SBNY), and Western Alliance Bancorporation (WAL) are investigated.

Additionally, we estimate the CARJIST model for a dataset consisting of five prominent commercial banks. Table 5 shows the parameter estimates of EGARCH(1,1) models, and table 6 provides the estimates for the parameters left. The first salient observation is the comparatively lower value of δ_i than that extracted from regional banks on average. This aligns with the intuition since these commercial banks have not undergone bankruptcy during the sample period. Moreover, the autocorrelation parameter a_l demonstrates the clustering of common jumps, whereas a_ϕ suggests a relatively lower persistency of the jump intensity. The cross-responsive parameter $b_{l,\phi}$ is greater than b_l, emphasizing that the likelihood of jumps in individual banks is augmented by simultaneous downturns among commercial banks.

Table 5: Parameter estimates of EGARCH(1,1) model for five regional banks. Bank of America Corporation (BAC), Citigroup Inc. (CITI), JP Morgan (JPM), U.S. Bancorp (USB) and Wells Fargo & Company (WFC) are investigated.

	BAC	CITI	JPM	USB	WF
θ	0.0009^{***}	0.0006^{***}	0.0010^{***}	0.0006^{***}	0.0004^{***}
α	0.95^{***}	0.97^{***}	0.97^{***}	0.96^{***}	0.97^{***}
β	0.11^{***}	0.11^{***}	0.09^{***}	0.15^{***}	0.10^{***}

* Denote significance level at the 10 % level.
** Denote significance level at the 5 % level.
*** Denote significance level at the 1 % level.

Table 6: Parameter estimates of the CARJIST model for five commercial banks. Bank of America Corporation (BAC), Citigroup Inc. (CITI), JP Morgan (JPM), U.S. Bancorp (USB) and Wells Fargo & Company (WFC) are investigated.

δ_{BAC}	0.663^{***}
δ_{CITI}	1.078^{***}
δ_{JPM}	0.800^{***}
δ_{USB}	1.192^{**}
δ_{WF}	1.204^{***}
θ	-0.050
$\bar{\phi}$	-0.555^{*}
$\bar{l}$	-1.488^{***}
a_ϕ	0.651^{***}
b_ϕ	0.834^{***}
a_l	0.130
b_l	0.120
$b_{\phi,l}$	0.507^{*}
$b_{l,\phi}$	0.268^{***}

* Denote significance level at the 10 % level.
** Denote significance level at the 5 % level.
*** Denote significance level at the 1 % level.

Figure 7 shows the dynamics of (a) the common jump intensity λ_t and (b) the triggering probability p_t of the five commercial banks. Consistent with our expectations from the persistence parameter, λ_t exhibits clustering, whereas p_t shows a relatively jagged pattern. We observe hikes in both model variables after the SVB

collapse. Indeed, the average level of λ_t in five days starting on Mar 10, 2023, is 3.76 times higher than the unconditional mean $\bar{\lambda}$, and the average level of p_t in five days starting on Mar 10, 2023, is 1.29 times higher than $\bar{p}$. Specifically, λ_t remains at a high level as it records higher values than $\bar{p}$ for nine successive days after Mar 9, 2023. It follows that the regional bank crisis intensifies the occurrence of common jumps in commercial banks.

This observation supports the conclusion drawn by Yousaf and Goodell (2023) regarding the adverse effects of the SVB collapse on the financial sector.

Similar to the regional banks, there was no significant increase in λ_t and p_t during the COVID-19 period.

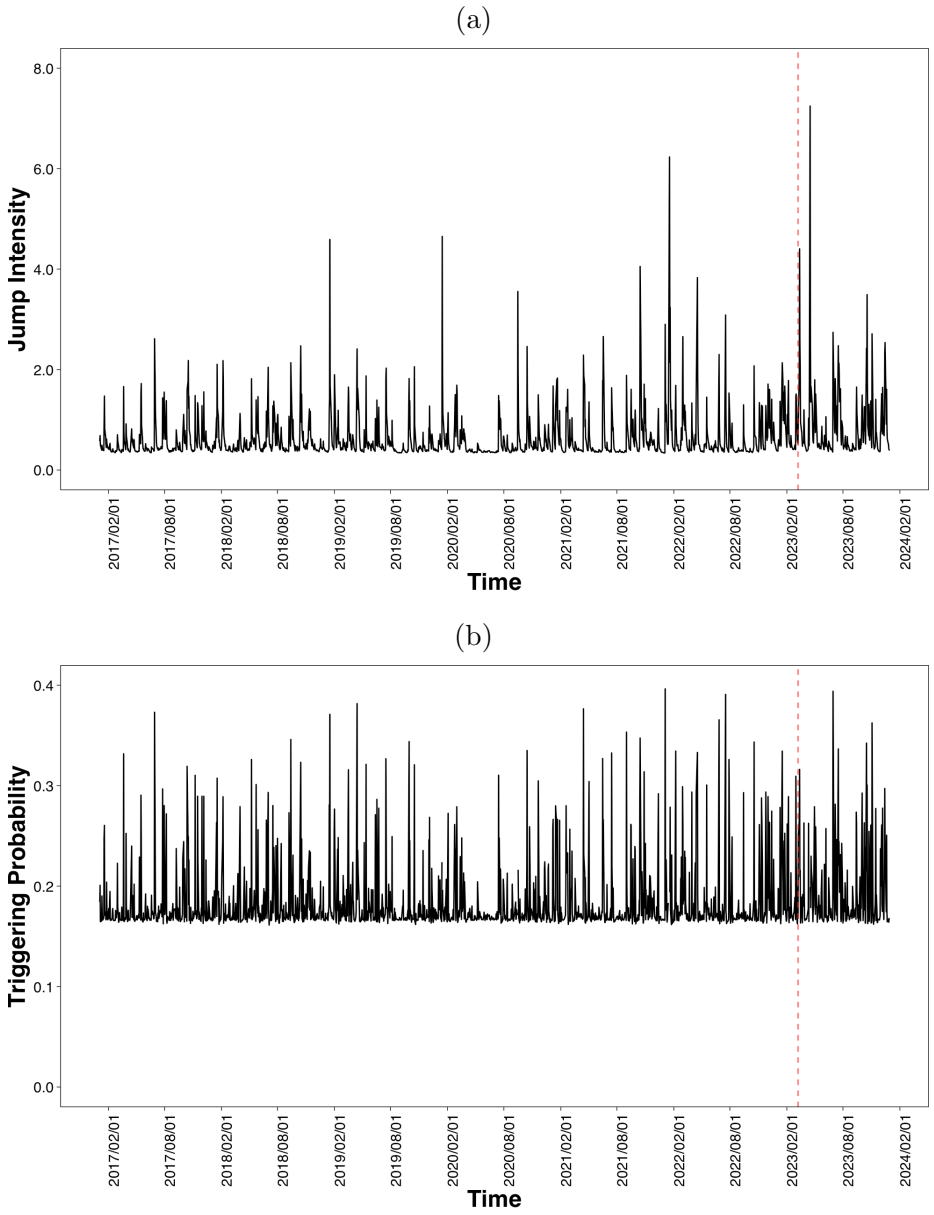

Figure 7: (a) jump intensity and (b) triggering probability of five commercial banks extracted from the CARJIST model. The red point represents the value on Mar 9, 2023.

Figure 8 provides the time-varying conditional volatilities of the five commercial banks. The blue line is the conditional volatility, and the black line is the EGARCH volatility. Conditional volatility reaches its peak at the onset of the COVID-19 pandemic, with the contribution of jump components being small. By comparing the blue and black lines, we observe infrequent deviation between the two lines. For instance, we observe simultaneous deviations on April 14, 2023. On this day, the quarterly earnings reports of CITI, WF, and USB are released, which impacts volatility. Furthermore, we observe deviations in all banks except for JPM on March 14, 2023, which we attribute to SVB collapse. Especially, both EGARCH and jump

components rise in USB around this day.

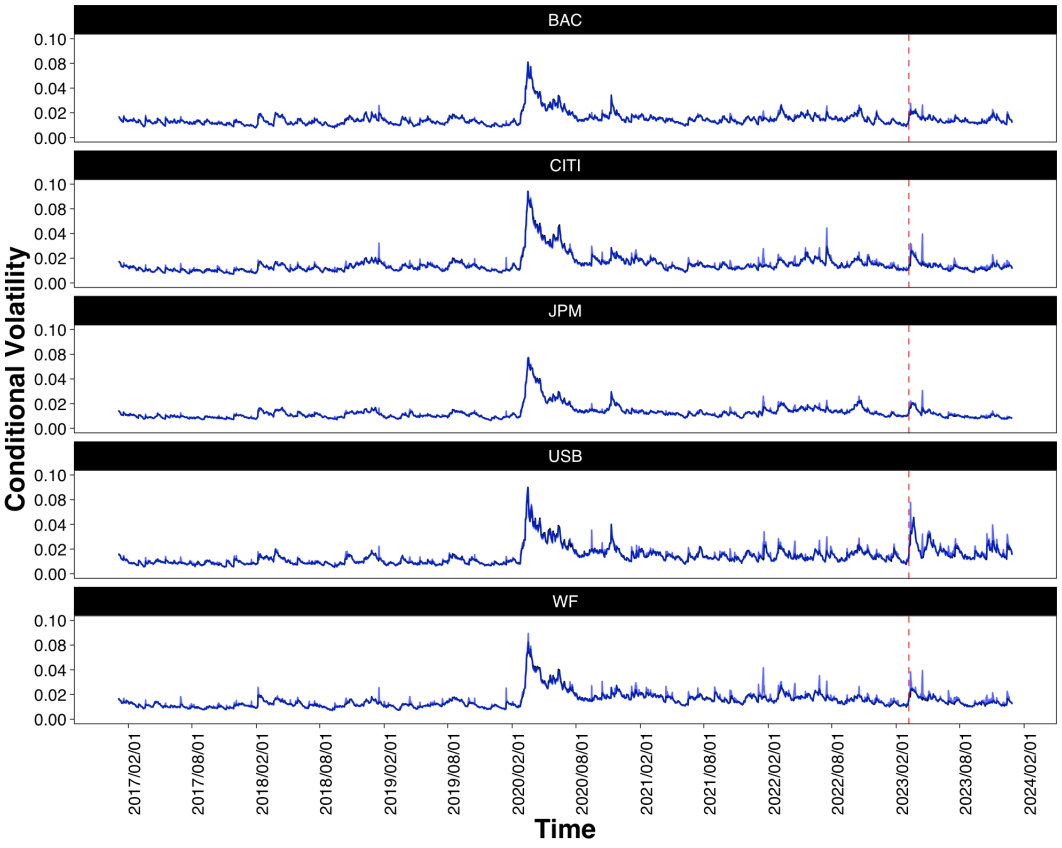

Figure 8: The time-varying conditional volatility of five commercial banks from the CARJIST model. The blue line is the conditional volatility, and the black line is the EGARCH volatility. The red line represents Mar 9, 2023. Bank of America Corporation (BAC), Citigroup Inc. (CITI), JP Morgan (JPM), U.S. Bancorp (USB) and Wells Fargo & Company (WFC) are investigated.

Figure 9 shows the (a) ex-ante and (b) ex-post probabilities that multiple jumps occur simultaneously across more than three commercial banks. The high magnitude of ex-ante and ex-post common jump probability around Mar 9, 2023, emphasizes the spillover from the crisis. In particular, there is an evident common jump on Mar 13, 2023. Table 7 displays the dates and associated news for days when the ex-post probability of common jumps exceeds 0.9. This table illustrates how common jumps relate to actual news.

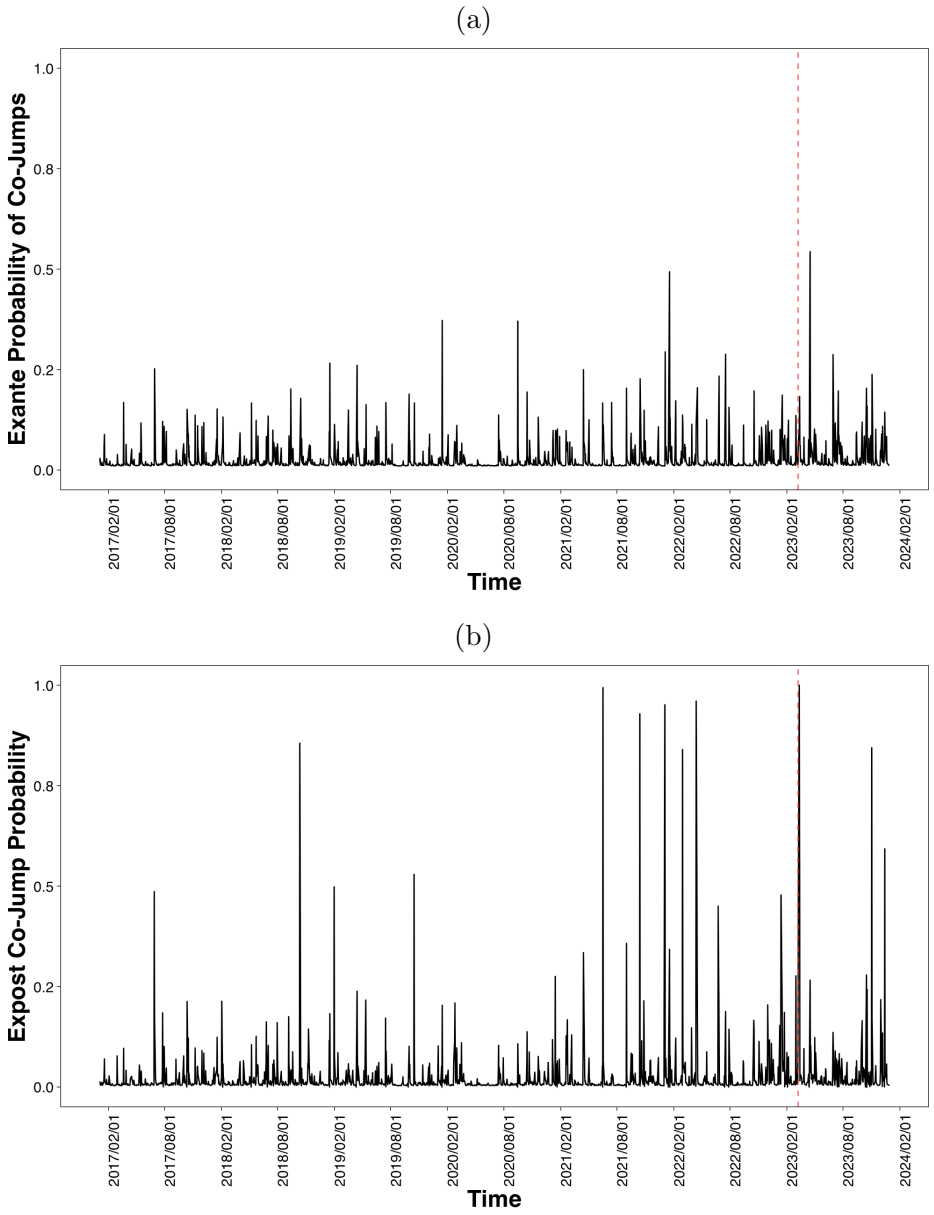

Figure 9: The (a) ex-ante and (b) ex-post probability that multiple jumps occur concurrently across more than three commercial banks. The red point represents the value on Mar 9, 2023.

Date	Prob.	Events
Jun 17, 2021	0.994	Fed announced two rate hikes for 2023
Oct 14, 2021	0.929	Quarterly Earnings Release of BAC, CITI, USB and WF.
Jan 03, 2022	0.951	The Year-End Santa Claus Rally.
Apr 14, 2022	0.960	Quarterly Earnings Release of CITI and WF, USB.
Mar 13, 2023	1.000	The Collapse of Silicon Valley Bank.

Table 7: Dates and associated events for days when the ex-post probability of common jumps exceeds 0.9

As a robustness check, we estimate an alternative specification of the CARJIST model for the regional banks. The driving force is scaled by the conditional variance without a square root operation. The results are detailed in Appendix B. Qualitative outcomes are consistent.

5.2 Interaction of Systemic Risks Between Regional Banks and Commercial Banks

We conduct a VAR analysis for the model variables of regional banks and large commercial banks to investigate whether the collapses of regional banks spread to commercial banks. In addition to the model variables, we include the risk-free rate, term spread, CBOE SKEW Index (SKEW) index, VIX, and economic policy uncertainty (EPU) index constructed by Baker et al. (2016). This analysis investigates the connection between model variables and major economic variables.

We employ the effective federal funds rate (FFR) as the risk-free rate. As a term spread, the difference between the 10-year Treasury constant maturity and the effective federal funds rate is utilized. SKEW index is provided by the Chicago Board Options Exchange (CBOE) designed to estimate the skewness of S&P 500 returns at the end of a 30-day horizon. The data on the effective federal funds rate and the term spread are available on the FRED, website of the Federal Reserve Bank of St. Louis [9]. The SKEW and VIX indices are downloaded from the website of CBoe. [10] The economic policy uncertainty index is downloaded from the website of Baker et al. (2016). [11]. Logarithms are taken for λ_{CML} and VIX. The logit sof p_{CML} and p_{REG} are used. The logarithm of λ_{REG} is detrended by using the autocorrelation parameter estimates reported in table 4. Subsequently, all data are normalized.

Table 8 provides the VAR(1) model estimates for the four model variables and five economic variables. Each row displays the coefficients corresponding to the variable named in the row for the variables specified by column names. Figure 10, 11a, and 11b depict the Impulse Response Functions (IRFs) with regard to significant coefficients.

The first noteworthy point is that the coefficients of λ_{REG} on λ_{CML} and p_{CML} are both statistically significant. To observe this effect visually, Figure 10 reports the IRFs of the intensity (left) and triggering probability (right) of commercial banks to a 1% shock in the intensity of regional banks. Indeed, 1% increment in the jump intensity λ_{REG} of regional banks corresponds to a subsequent increase of 51.7% in the jump intensity λ_{CML} of commercial banks relative to its unconditional mean, and an increase of 2.77% in the triggering probability p_{CML} of commercial banks relative to its unconditional mean. It suggests that individual crashes in the regional banks amplify the risk of unusual jump events and co-movements in commercial banks.

[9] Effective Federal Funds Rate [EFFR] and 10-Year Treasury Constant Maturity Minus Federal Funds Rate [T10YFF] are retrieved from FRED, Federal Reserve Bank of St. Louis; https://fred.stlouisfed.org/series/EFFR, February 20, 2023.

[10] The SKEW index and VIX are retrieved from the website of the Chicago Board Options Exchange; https://www.cboe.com/us/indices/dashboard/skew/, February 20, 2023.

[11] The economic policy uncertainty index constructed by Baker et al. (2016) is downloaded from their website; https://www.policyuncertainty.com/, February 20, 2023.

Hence, considering regional banks is crucial for the risk management of portfolios consisting of commercial banks. Furtheremore, λ_{COM} positively affects λ_{REG} and p_{REG}. This suggests that the contagion in commercial banks also spreads to regional banks.

In contrast to λ_{COM}, there are no significant effects of p_{COM} on λ_{REG} or p_{REG}. Similary, p_{REG} has no significant effect on λ_{COM} and p_{COM}. Thus, the change in interconnectedness among commercial banks does not propagate to the regional banks, and vice versa.

We observe significant positive coefficients of FFR on λ_{REG}, p_{REG}, λ_{COM}, p_{REG}. It is helpful to see the IRFs of the intensity (left) and triggering probability (right) to a 1% shock in the FFR, as shown in Figure 11a. Indeed, 1% absolute increase in FFR leads to a subsequent increase of 0.30% in λ_{REG} and 1.20% in p_{REG}, both relative to its unconditional mean. This translates to a 3.54% rise in the common jump probability relative to its average level. [12] As for commercial banks, 1% absolute increase in FFR leads to a subsequent increase of 2.44% in λ_{REG} and 1.11% in p_{CML}, both relative to its unconditional mean. This leads to a 4.77% elevation in the common jump probability relative to the average level. These findings suggest that an increase in the FFR level substantially amplifies the likelihood of common jump occurrences in both regional and commercial banks.

Moreover, the coefficients of the term spread on λ_{REG} and p_{REG} are significantly negative. The IRFs of the intensity (left) and triggering probability (right) to a 1% shock in the term spread are described in Figure 11b. Specifically, 1% absolute decrease in the term spread leads to a subsequent relative increase of 6.43% in λ_{REG} and 19.7% in p_{REG}, resulting in a 59.1% increase in common jump probability. Hence, the rise in short-term rates compared with long-term rates notably leads to tail events in regional banks. For commercial banks, the coefficients on λ_{COM}, p_{COM} are also significant. As can be seen in the IRFs, a 1% absolute increase in the term spread results in a relative increase of 31.5% in λ_{CML} and 13.8% in p_{CML}, triggering a 60.3% increase in the common jump probability.

Drawing upon the impulse of both the FFR and term spread, our findings corroborate the conclusions of studies such as Metrick (2024), Chang et al. (2023), and Jiang et al. (2023). These studies suggest that the rapid monetary tightening initiated in Q1 2022 in the U.S. reduces banks' assets and exacerbates concerns among uninsured depositors regarding bank default risk, ultimately precipitating solvency runs.

It is interesting to note that the response to the term spread decreases more rapidly than the response to FFR for both regional and commercial banks. Therefore, an increase in the term spread predicts a decrease in the shorter-term tail risk, whereas the FFR level predicts longer-term tail risk. Additionally, based on figures 11a and 11b, we note that the reaction in intensity is more pronounced for regional banks in response to the impulse in FFR and term spread, whereas the response in triggering probability is more pronounced for commercial banks. This underscores different reactions to interest rate changes based on bank size.

The SKEW index increases the p_{REG}, which demonstrates the relationship be-

[12] The average level of the common jump probability is calculated given λ_{REG} and p_{REG}.

tween contagion in regional banks and tail risk in the $S\&P500$ index. Moreover, λ_{COM} and p_{COM} predict the SKEW index positively, indicating that stress in commercial banks influences financial markets. Conversely, regional banks exhibit a weaker market impact.

Table 8: Parameter estimates of VAR(1) model with constant. λ_{REG} and p_{REG} represent the common jump intensity and triggering probability of regional banks, whereas λ_{CML} and p_{CML} represent those of commercial banks. FFR represents the effective federal funds rate, the TermSP refers to the term spread between the 10-year yield and the effective federal funds rate. SKEW is the SKEW Index as provided by the CBOE, and EPU is the economic policy uncertainty index. A logarithm is taken for VIX and λ_{CML}. The logit is computed for p_{REG} and p_{CML}. λ_{REG} is detrended after the logit transformation. All data are normalized.

	λ_{REG}	p_{REG}	λ_{CML}	p_{CML}	FFR	TermSP	SKEW	VIX	EPU
Constant	0.000	-0.000	-0.000	-0.000	0.002**	0.001	0.000	0.000	-0.000
AR(1) matrix									
λ_{REG}	-0.009	-0.008	0.077***	0.100***	-0.001	0.001	-0.004	0.006	-0.005
p_{REG}	-0.058*	0.831***	-0.023	-0.030	0.001	-0.033	0.008	-0.002	-0.016
λ_{CML}	0.136***	0.064***	0.620***	-0.040	-0.002	-0.004	-0.023*	0.009	-0.024
p_{CML}	-0.047	-0.021	0.020	0.157***	0.001	0.029	0.022*	-0.002	0.028
FFR	0.069**	0.050***	0.082***	0.104***	1.000***	-0.011	-0.013	-0.007	-0.034*
TermSP	-0.065***	-0.037***	-0.048***	-0.058**	-0.001	0.030	-0.010	0.010*	-0.003
SKEW	0.043	0.035***	0.050**	0.065**	-0.001	0.053**	0.946***	-0.003	0.029*
VIX	0.018	0.014	0.037	0.046	-0.000	0.053*	-0.018*	0.970***	0.232***
EPU	-0.029	-0.008	-0.027	-0.036	-0.001	-0.045	0.007	0.008	0.606***

* Denote significance level at the 10 % level.
** Denote significance level at the 5 % level.
*** Denote significance level at the 1 % level.

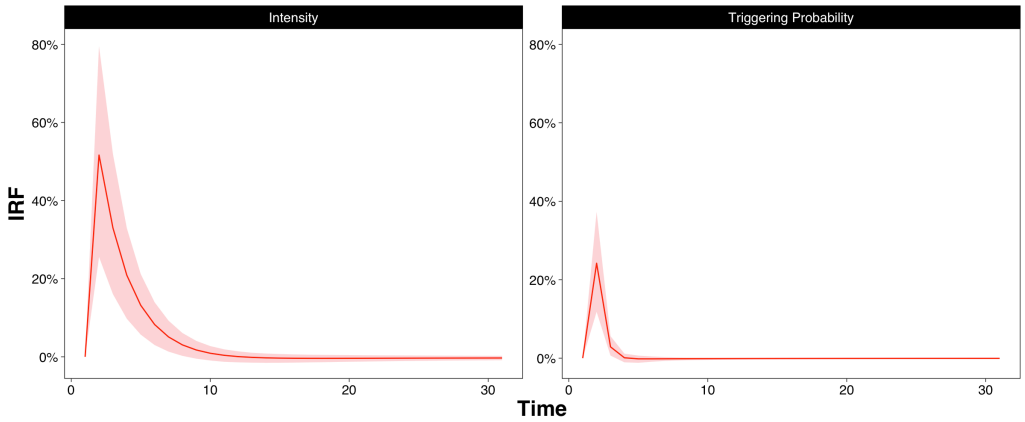

Figure 10: Impulse Response Functions of the intensity (left) and triggering probability (right) of commercial banks to a 1% shock in the intensity of regional banks.

(a) IRFs to a 1% shock in the FFR.

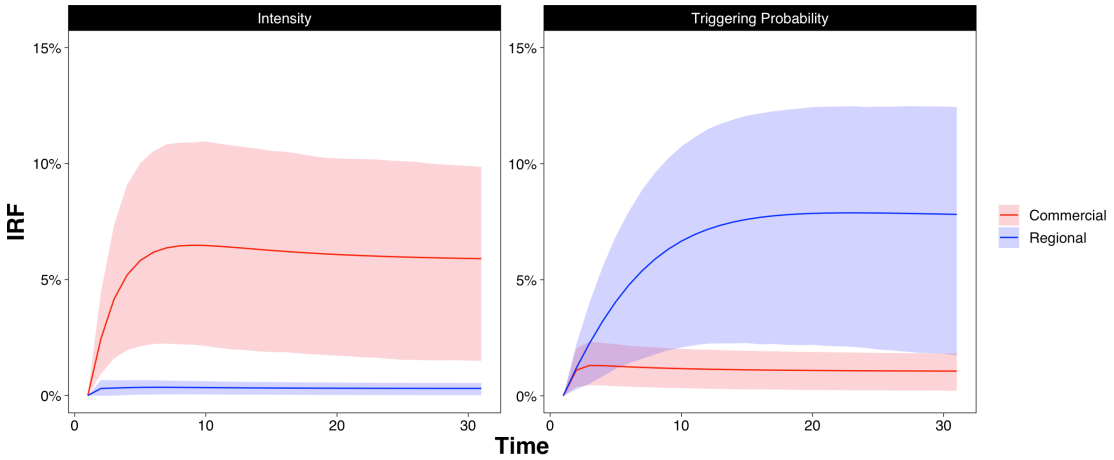

(b) IRFs to a 1% shock in the term spread.

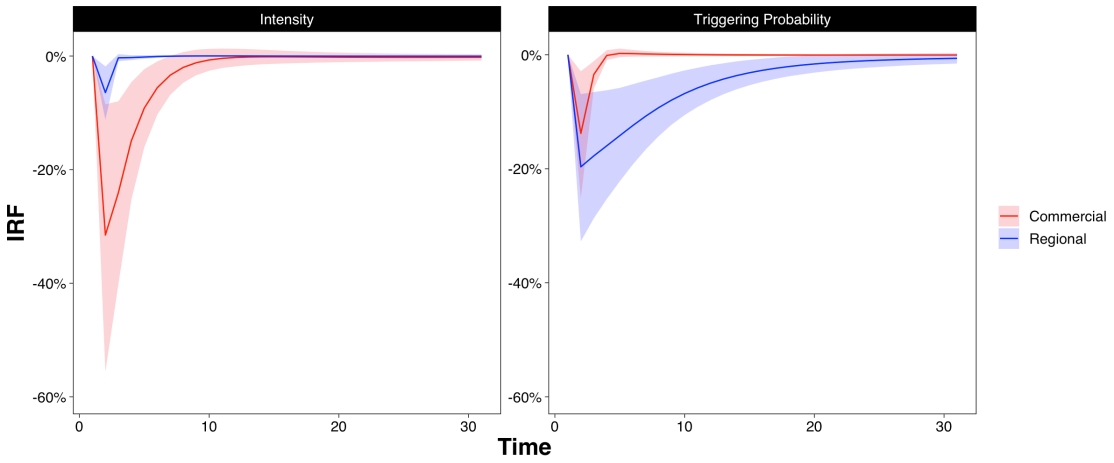

Figure 11: Impulse Response Functions of the intensity (left) and triggering probability (right) to a 1% shock in the FFR (top) and in the term spread (bottom). The red and blue lines represent the impulses of commercial banks and regional banks, respectively. The shaded areas are 95% confidential intervals.

In addition, we explore the relationship between systemic risk in the banking industry and deposits. To accomplish this, we aggregate the model variables by computing weakly means and conduct a VAR analysis with deposit amounts. The weekly deposit data of all commercial banks in the U.S. are retrieved from the FRED. [13] We take the log difference of the deposit. Table 9 shows the parameter estimates.

The coefficient of deposits on λ_{REG} is significantly negative, whereas that on p_{REG} is not significant. Withdrawals of deposits increase systemic risk but may not necessarily spread. On the other hand, the level of deposit affects both λ_{COM} and p_{COM}, indicating that withdrawals lead to tail events in commercial banks.

[13]Board of Governors of the Federal Reserve System (U.S.), Deposits, All Commercial Banks [DPSACBW027SBOG], retrieved from FRED, Federal Reserve Bank of St. Louis; https://fred.stlouisfed.org/series/DPSACBW027SBOG, March 6, 2024.

Table 9: Parameter estimates of weekly VAR model.

	λ_{REG}	p_{REG}	λ_{CML}	p_{CML}	Deposit
Constant	0.003	-0.001	-0.001	0.000	-0.001
AR(1) matrix					
λ_{REG}	0.039	0.355^{***}	0.015	-0.011	-0.022
p_{REG}	-0.089	0.343^{***}	0.058	0.061	-0.026
λ_{CML}	0.231^{*}	0.231^{**}	-0.134	-0.036	-0.065
p_{CML}	-0.120	-0.108	0.404^{***}	-0.005	0.030
Deposit	-0.095^{*}	-0.054	-0.095^{*}	-0.096^{*}	0.274^{***}

* Denote significance level at the 10 % level.
** Denote significance level at the 5 % level.
*** Denote significance level at the 1 % level.

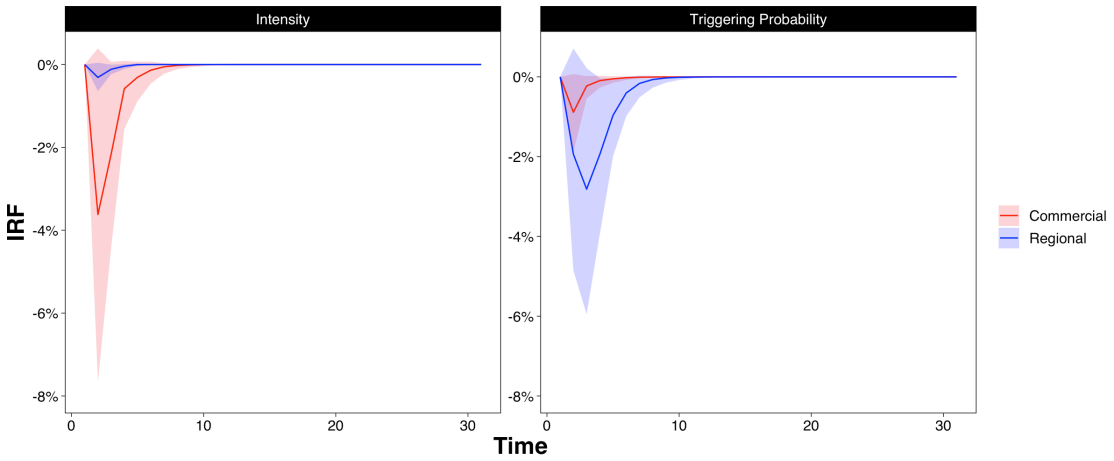

Figure 12: Impulse Response Functions of the intensity (left) and triggering probability (right) of commercial banks to a one-standard-deviation shock in the deposit.

Table 8 and Table 9 offer complementary insights. Notably, different economic variables predict the two model variables. While the common jump intensity λ_{REG} is primarily influenced by a macroeconomic fundamental factor, namely depositor withdrawals induced by perceived risks in the banking sector, the triggering probability is more closely linked to the risk appetite of investors, as evidenced by its correlation with the SKEW index. This highlights that λ_{REG} and p_{REG} characterize the different structures of the time series: systemic risk and ripple effect, respectively.

5.3 Network Systemic Risk Among Regional Banks

We investigate the directional tail co-movement across the network of regional banks using the systemic risk measure ΔCoVaR proposed by Tobias and Brunnermeier

(2016). ΔCoVaR is the change in the Value at Risk of institution j conditional on institution i being under distress relative to its median state. This measure allows us to quantify tail co-movements in the sense that distress in institution i affects the probability of institution j being distressed.

We denote the return of institution i as r_i. $\text{CoVaR}_q^{j|C(r_i)}$ is the VaR of institution j conditional on the state of institution i satisfying

$$\Pr(r_j = \text{CoVaR}_q^{j|C(r_i)} | C(r_i)) = q \tag{5.1}$$

where $C(r_i)$ is some events of institution i, and q is the quantile. We define $\text{CoVaR}_q^{j|i}$ as the VaR of commercial bank j given the condition that the return loss of institution i exceeds its VaR.

$$\Pr(r_j \leq \text{CoVaR}_q^{j|i} | r_i = -\text{VaR}_q^i) = q \tag{5.2}$$

where VaR_q^i is the VaR of institution i with the q-quantile. As a benchmark state, we use $C(r_i) = \{r_i = -\text{VaR}_{0.5}^i\}$ and introduce $\text{CoVaR}_q^{j|\text{Med}(i)}$ as

$$\Pr(r_j \leq \text{CoVaR}_q^{j|\text{Med}(i)} | r_i = -\text{VaR}_{0.5}^i) = q. \tag{5.3}$$

The systemic risk measure $\Delta\text{CoVaR}_q^{j|i}$ is defined as

$$\Delta\text{CoVaR}_q^{j|i} = \text{CoVaR}_q^{j|i} - \text{CoVaR}_q^{j|\text{Med}(i)}. \tag{5.4}$$

We start with computing the VaR and CoVaR based on EGARCH-filtered returns. Subsequently, to estimate the VaR and CoVaR of raw returns, we multiply the VaR and CoVaR of the EGARCH-filtered returns by the conditional volatility. Let $\tilde{\text{VaR}}_{q,t}^i$ be the VaR of the EGARCH-filtered return of institution i at time t. Following this definition, it is acquired by numerically solving

$$\int_{-\infty}^{-\tilde{\text{VaR}}_{q,t}^i} f(\epsilon_{i,t}|\mathcal{F}_{t-1}) d\epsilon_{i,t} = q \tag{5.5}$$

where $f(\epsilon_{i,t}|\mathcal{F}_{t-1})$ is a marginal conditional distribution of the EGARCH-filtered return $\epsilon_{i,t}$. The marginal conditional distribution is easily computed from the linearity of the likelihood in Section 3.8. For instance, consider the case of calculating the marginal conditional distribution of asset 1:

$$\begin{aligned} f(\epsilon_{1,t}|\mathcal{F}_{t-1}) &= \int_{\mathcal{R}^{N-1}} f(\boldsymbol{\epsilon}_t|\mathcal{F}_{t-1}) d\epsilon_{2,t} \cdots d\epsilon_{N,t} \\ &= \sum_{j=0}^{\infty} \sum_{g_1=0}^{1} \int_{\mathcal{R}^{N-1}} \sum_{g_2=0}^{1} \cdots \sum_{g_N=0}^{1} f_{t,j,\mathbf{g}} d\epsilon_{2,t} \cdots d\epsilon_{N,t} \\ &= \sum_{j=0}^{\infty} \sum_{g_1=0}^{1} f(\epsilon_{1,t}|\mathcal{F}_{t-1}, n_t = j, b_{1,t} = g_1) p(n_t = j|\mathcal{F}_{t-1}) p(b_{1,t} = g_1|\mathcal{F}_{t-1}). \end{aligned} \tag{5.6}$$

Then, the VaR of the raw return of institution i at time t is

$$\text{VaR}_{q,t}^i = \sigma_{i,t} \tilde{\text{VaR}}_{q,t}^i. \tag{5.7}$$

We denote the CoVaR of the EGARCH-filtered return of the institution j conditional on i's distress as $\text{Co}\tilde{\text{V}}\text{aR}_{q,t}^{j|i}$. Given $\tilde{\text{VaR}}_{q,t}^{i}$, we calculate $\text{Co}\tilde{\text{V}}\text{aR}_{q,t}^{j|i}$ by numerically solving

$$\frac{\int_{-\infty}^{-\text{Co}\tilde{\text{V}}\text{aR}_{q,t}^{j|i}} \int_{-\infty}^{-\tilde{\text{VaR}}_{q,t}^{i}} f(\epsilon_{i,t}, \epsilon_{j,t}|\mathcal{F}_{t-1}) d\epsilon_{i,t} d\epsilon_{j,t}}{q} = q \tag{5.8}$$

where q is the quantile. The conditional bivariate distribution $f(\epsilon_{i,t}, \epsilon_{j,t}|\mathcal{F}_{t-1})$ can be calculated as we do in the computation of $\tilde{\text{VaR}}_{q,t}^{i}$. By multiplying the conditional volatility, we have the CoVaR of the raw return of the institution j conditional on i's distress.

$$\text{CoVaR}_{q,t}^{j|i} = \sigma_{j,t} \text{Co}\tilde{\text{V}}\text{aR}_{q,t}^{j|i}. \tag{5.9}$$

$\text{CoVaR}_{q,t}^{j|\text{Med}(i)}$ is estimated in the same manner. $\Delta\text{CoVaR}_{q,t}^{j|i}$ is calculated by pludging $\text{CoVaR}_{q,t}^{j|i}$ and $\text{CoVaR}_{q,t}^{j|\text{Med}(i)}$ into 5.4.

Based on the parameter estimates in table 6, we estimate the dynamic network $\Delta\text{CoVaR}_{q,t}^{j|i}$ for all pairs of the five regional banks. Table 10a shows the mean of $\Delta\text{CoVaR}_{q}^{j|i}$ before and after Mar 9 of 2023 for the institutions listed in the **FROM** column conditioned on the institutions in the **TO** column. The rows are organized in ascending order based on the magnitude of $\Delta\text{CoVaR}_{q}^{j|i}$. SVB and SBNY record high $\Delta\text{CoVaR}_{q}^{j|i}$s both before and after Mar 9, 2023. FRCB attains elevated positions after March 9, 2023, suggesting that FRCB becomes susceptible to severe shocks when conditioned on the distress of other institutions following the regional bank turmoil. $\Delta\text{CoVaR}_{q}^{j|i}$ to FFWM and WAL become relatively lower owing to low conditional volatilities.

FROM	TO	$\Delta\text{CoVaR}_q^{j\|i}$
WAL	SVB	0.076
FFWM	SVB	0.066
WAL	SBNY	0.056
FRCB	SVB	0.054
SBNY	SVB	0.051
FFWM	SBNY	0.049
SVB	WAL	0.047
SBNY	WAL	0.042
FFWM	WAL	0.042
FRCB	SBNY	0.042
FRCB	WAL	0.042
SVB	SBNY	0.041
WAL	FRCB	0.037
WAL	FFWM	0.035
FFWM	FRCB	0.032
SVB	FRCB	0.030
SVB	FFWM	0.028
SBNY	FRCB	0.028
FRCB	FFWM	0.028
SBNY	FFWM	0.028

(a)

FROM	TO	$\Delta\text{CoVaR}_q^{j\|i}$
FFWM	SBNY	0.797
WAL	SBNY	0.729
FFWM	SVB	0.635
WAL	SVB	0.582
FRCB	SBNY	0.460
FFWM	FRCB	0.389
WAL	FRCB	0.360
FRCB	SVB	0.330
SBNY	SVB	0.311
SBNY	FRCB	0.226
SVB	SBNY	0.137
SVB	FRCB	0.105
FFWM	WAL	0.070
WAL	FFWM	0.070
FRCB	FFWM	0.061
FRCB	WAL	0.060
SBNY	FFWM	0.060
SBNY	WAL	0.060
SVB	WAL	0.051
SVB	FFWM	0.049

(b)

Table 10: Network $\Delta\text{CoVaR}_q^{j|i}$ (a) before and (b) after Mar 9, 2023. First Foundation Inc. (FFWM), First Republic Bank (FRCB), SVB Financial Group (SVB), Signature Bank (SBNY) and Western Alliance Bancorporation (WAL) are investigated.

Figure 13 visualize the table 10 in a network plot. The blue shade deepens overall after Mar 9, 2023, symbolizing a strengthening interconnectedness among regional banks attributed to the SVB run. In particular, arrows to SVB, SBNY and FRCB stand out. These banks experience bankruptcy, initiating pronounced mutual excitements, consequently triggering the contagion within regional banks. Our CARJIST model offers precise insights into tail contagion by characterizing abnormal and extreme events as common jumps. This is a departure from the GARCH-type methodology, which treats such events as correlated normal shocks.

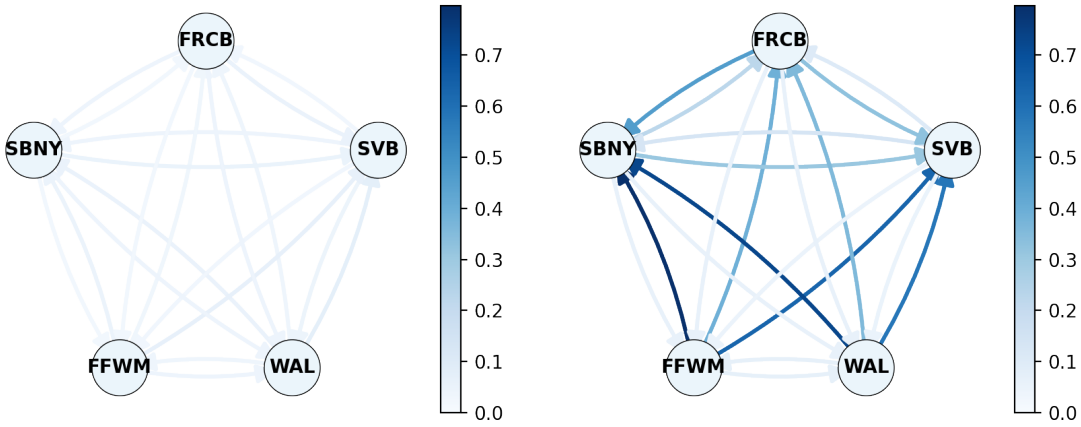

(a) (b)

Figure 13: Network plot of $\Delta\text{CoVaR}_q^{j|i}$ (a) before and (b) after Mar 9, 2023. First Foundation Inc. (FFWM), First Republic Bank (FRCB), SVB Financial Group (SVB), Signature Bank (SBNY) and Western Alliance Bancorporation (WAL) are investigated.

5.4 Did the Risk of Silicon Valley Bank Failure Spread to Commercial Banks?

To analyze the risk in commercial banks induced by the regional banks' run, we estimate the six-dimensional version of our CARJIST model for BAC, CITI, JPM, USB, WF, and SVB and estimate the time-varying CoVaR denoted as $\Delta\text{CoVaR}_{q,t}^{j|i}$. Parameter estimates are listed in Appendix C.

Figure 14 shows the unconditional VaR with quantile $q = 0.01$ estimated from the CARJIST model. The relative size of VaR is governed by the conditional volatility $\sigma i, t$, the individual jump size δ_i and the correlation with SVB. The first observation is the boost in VaRs in March 2022 due to the COVID-19 shock. Another sharp rise in VaR is observed on Mar 10, 2023, when the regional banking crisis begins. In particular, USB records the highest VaR on this day.

Figure 15 shows $\text{CoVaR}_{0.01,t}^{j|\text{SVB}}$, which reveals observations similar to VaR.

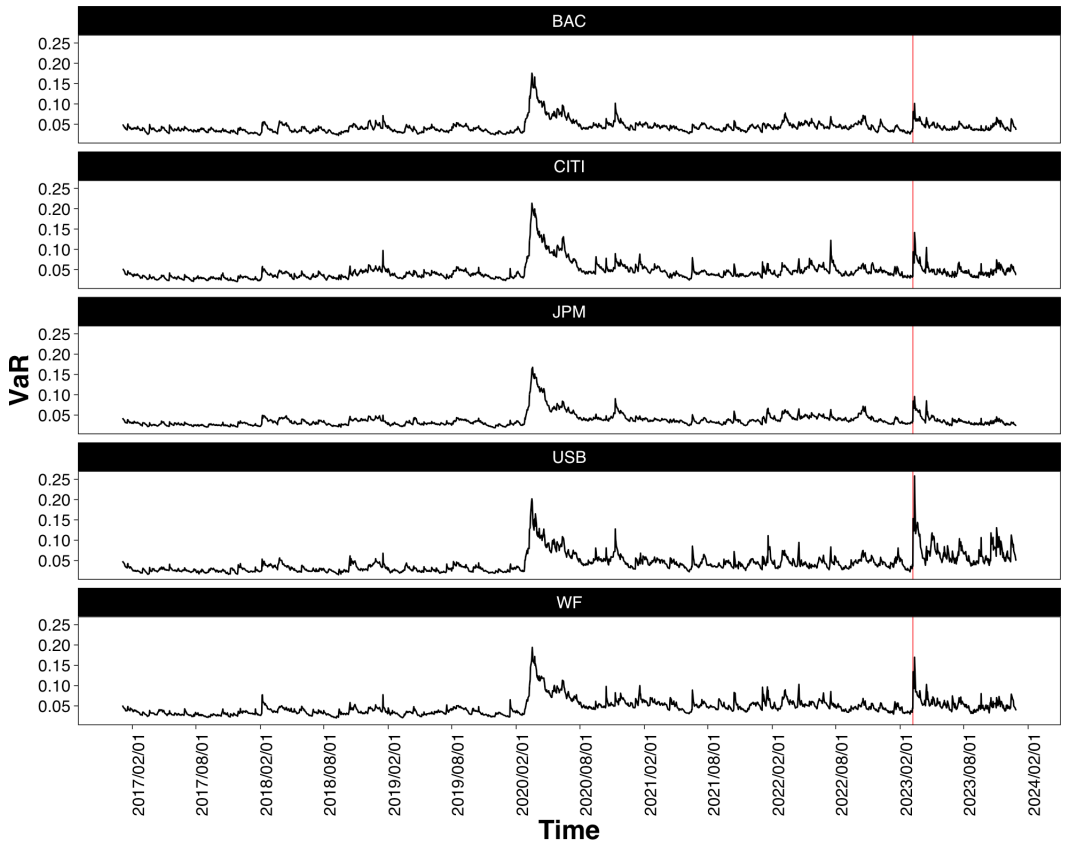

Figure 14: VaR of five commercial banks derived from the CARJIST model. The red line represents Mar 10, 2023. Bank of America Corporation (BAC), Citigroup Inc. (CITI), JP Morgan (JPM), U.S. Bancorp (USB) and Wells Fargo & Company (WFC) are investigated.

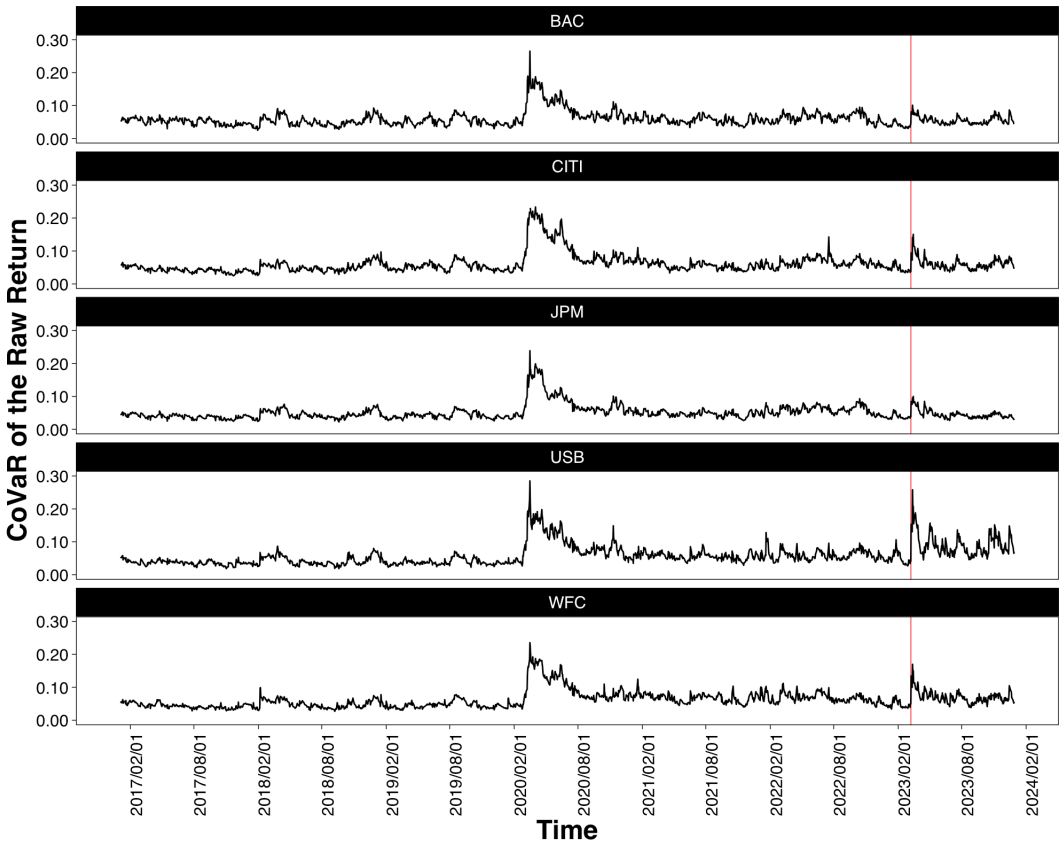

Figure 15: $\text{CoVaR}_{0.01,t}^{j|\text{SVB}}$ of five commercial banks conditional on SVB derived from the CARJIST model. The red point represents Mar 9, 2023. Bank of America Corporation (BAC), Citigroup Inc. (CITI), JP Morgan (JPM), U.S. Bancorp (USB) and Wells Fargo & Company (WFC) are investigated.

Figure 16 shows the $\Delta\text{CoVaR}_{q,t}^{j|\text{SVB}}$ with $q = 0.01$ based on the estimated CARJIST model. As shown in the figure, $\Delta\text{CoVaR}_{0.01,t}^{j|\text{SVB}}$ gains for all commercial banks around the regional bank crisis. Especially, USB achieves high values of $\Delta\text{CoVaR}_{0.01,t}^{j|\text{SVB}}$ around Mar 10, 2023. These outcomes substantiate that SVB plays a significant role in augmenting the tail risk in commercial banks, with the evidence indicating a more pronounced tail co-movement between SVB and USB. The highest level of $\Delta\text{CoVaR}_{0.01,t}^{j|\text{SVB}}$ are observed in March 2020 in all commercial banks. This is mainly because of the high conditional volatility during the turmoil induced by the COVID-19 pandemic.

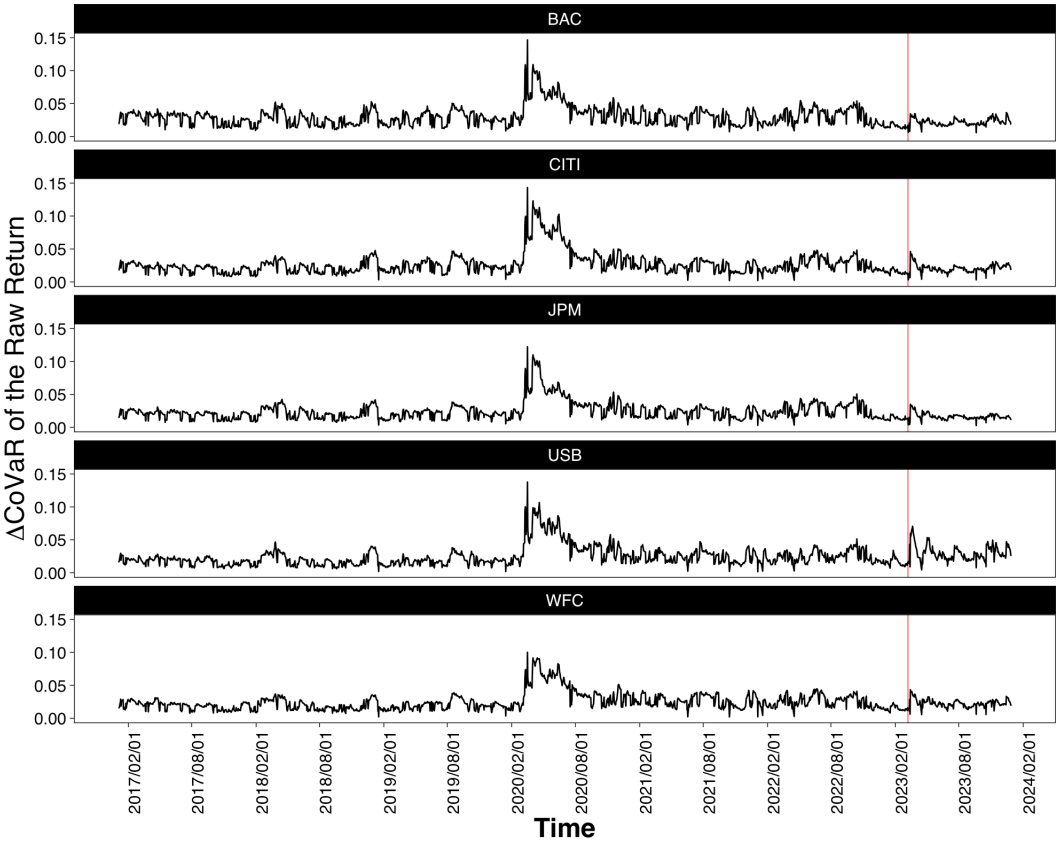

Figure 16: $\Delta\text{CoVaR}^{j|\text{SVB}}_{0.01,t}$ of five commercial banks conditional on SVB derived from the CARJIST model. The red line represents Mar 9, 2023. Bank of America Corporation (BAC), Citigroup Inc. (CITI), JP Morgan (JPM), U.S. Bancorp (USB) and Wells Fargo & Company (WFC) are investigated.

Table 11 summarizes the descriptive statistics of $\Delta\text{CoVaR}^{j|\text{SVB}}_{0.01,t}$ for samples of before and after SVB meltdown. The pre-period is delineated as the 30 trading dates preceding March 9, 2023, whereas the post-period encompasses the thirty trading dates following March 9, 2023, inclusive of this day. For all commercial banks under investigation, the means of $\Delta\text{CoVaR}^{j|\text{SVB}}_{0.01,t}$ after the SVB failure is greater than that in the pre-period. [14] Especially, the USB shows the highest mean in the post-SVB period.

This phenomenon may be attributed to the relatively smaller size of USB among the five commercial banks examined, which results in weaker inflows of deposits from flight-to-safety investors.

[14]The result is unchanged when the window size is fifteen days and sixty days.

	BAC	CITI	JPM	USB	WF
Before					
Mean	0.0152	0.0150	0.0136	0.0167	0.0151
Std. Dev.	0.003	0.003	0.002	0.006	0.004
Skewness	0.870	1.172	1.200	0.948	0.963
Min	0.012	0.011	0.011	0.009	0.011
Max	0.022	0.023	0.020	0.034	0.024
After					
Mean	0.0242	0.0249	0.0210	0.0355	0.0266
Std. Dev.	0.008	0.012	0.009	0.020	0.010
Skewness	-0.754	-0.073	-0.274	0.290	-0.362
Min	0.006	0.003	0.004	0.004	0.006
Max	0.035	0.046	0.035	0.071	0.043

Table 11: Descriptive statistics of CoVaR time-series of commercial banks given Silicon Valley Bank (SVB). Bank of America Corporation (BAC), Citigroup Inc. (CITI), JP Morgan (JPM), U.S. Bancorp (USB) and Wells Fargo & Company (WFC) are investigated.

6 Conclusion

In this paper, we study whether and how SVB collapse has impacted major regional banks' stock dynamics. Specifically, we explicitly model common jumps with time-varying jump intensity and triggering probability to capture the systemic risk and ripple effect, respectively. We empirically estimate the model for five regional banks and five large commercial banks. Using the two model variables extracted from the model, we study the financial variables that interact with crisis risk. Our main findings are as follows: First, both the systemic risk and ripple effect for the regional banks are different from those of the large commercial banks. Second, we find that systemic risk in regional banks and large commercial banks amplify each other. Moreover, the Federal Funds rate and term spread significantly impact the systemic risk and ripple effect for the regional banks. Third, we compute CoVaR and demonstrate that the CoVaR co-movements for regional banks have become stronger during the SVB failure period than during the pre-SVB failure period.

There are several topics for future research in this area. First, it would be interesting to investigate the relationship between CoVaR and a firm's fundamentals. In this research, we focus on computing the CoVaR to illustrate the change in co-movements among banks. Extending this approach, researchers could explore the fundamental variables that predict future risk, as captured by CoVaR. Second, it would be worthwhile to extend the CARJIST model to include a large number of assets. The current model maintains a manageable number of parameters, accommodating the heterogeneity of jumps across assets through the triggering probability. However, when dealing with large cross-sectional datasets, the likelihood computation requires substantial computational resources. An alternative specification,

which offers both flexibility and ease of estimation, would expand its empirical applicability.

References

Acharya, V. V., M. P. Richardson, K. L. Schoenholtz, B. Tuckman, R. Berner, S. G. Cecchetti, S. Kim, S. Kim, T. Philippon, S. G. Ryan, et al. (2023). Svb and beyond: The banking stress of 2023. *Available at SSRN 4513276*.

Aït-Sahalia, Y., J. Cacho-Diaz, and R. J. Laeven (2015). Modeling financial contagion using mutually exciting jump processes. *Journal of Financial Economics 117*(3), 585–606.

Baker, S. R., N. Bloom, and S. J. Davis (2016). Measuring economic policy uncertainty. *The quarterly journal of economics 131*(4), 1593–1636.

Ballestra, L. V., E. D'Innocenzo, A. Guizzardi, et al. (2023). Score-driven modeling with jumps: An application to s&p500 returns and options. *Journal of Financial Econometrics*, 1–32.

Blasques, F., P. Gorgi, and S. J. Koopman (2021). Missing observations in observation-driven time series models. *Journal of Econometrics 221*(2), 542–568.

Brownlees, C., B. Chabot, E. Ghysels, and C. Kurz (2020). Back to the future: Backtesting systemic risk measures during historical bank runs and the great depression. *Journal of Banking & Finance 113*, 105736.

Chang, B., I.-H. Cheng, and H. G. Hong (2023). The fundamental role of uninsured depositors in the regional banking crisis. *Available at SSRN 4507551*.

Choi, D. B., P. Goldsmith-Pinkham, and T. Yorulmazer (2023). Contagion effects of the silicon valley bank run. Technical report, National Bureau of Economic Research.

Creal, D., S. J. Koopman, and A. Lucas (2013). Generalized autoregressive score models with applications. *Journal of Applied Econometrics 28*(5), 777–795.

Das, S. R. and R. Uppal (2004). Systemic risk and international portfolio choice. *The Journal of Finance 59*(6), 2809–2834.

Girardi, G. and A. T. Ergün (2013). Systemic risk measurement: Multivariate garch estimation of covar. *Journal of Banking & Finance 37*(8), 3169–3180.

Jiang, E. X., G. Matvos, T. Piskorski, and A. Seru (2023). Monetary tightening and us bank fragility in 2023: Mark-to-market losses and uninsured depositor runs? Technical report, National Bureau of Economic Research.

Li, C. and J. M. Maheu (2020). A multivariate garch-jump mixture model.

Maheu, J. M. and T. H. McCurdy (2004). News arrival, jump dynamics, and volatility components for individual stock returns. *The Journal of Finance 59*(2), 755–793.

Mardia, K. V. (1970). Measures of multivariate skewness and kurtosis with applications. *Biometrika 57*(3), 519–530.

Metrick, A. (2024). The failure of silicon valley bank and the panic of 2023. *Journal of Economic Perspectives 38*(1), 133–152.

Tobias, A. and M. K. Brunnermeier (2016). Covar. *The American Economic Review 106*(7), 1705.

Yousaf, I. and J. W. Goodell (2023). Responses of us equity market sectors to the silicon valley bank implosion. *Finance Research Letters 55*, 103934.

A Model Description

A.1 Derivation of the Driving Force of ϕ_t.

The driving force of ϕ_t is calculated as

$$\begin{aligned}\tilde{s}_t^{\phi} &= \sum_{j=0}^{\infty}\sum_{\mathbf{g}\in\mathcal{G}_N}\frac{f_{t,j,\mathbf{g}}}{f(\boldsymbol{\epsilon}_t|\mathcal{F}_{t-1})}\frac{\nabla_{t,j,\mathbf{g}}^{\phi}}{\sqrt{\mathrm{Var}(\nabla_{t,j,\mathbf{g}}^{\phi}|\mathcal{F}_{t-1})}}\\ &= \frac{E(n_t|\mathcal{F}_t)-\lambda_t}{\sqrt{\lambda_t+\theta^2\lambda_t^2E(\mathbf{g}^T\Sigma_{t,j,\mathbf{g}}^{-1}\mathbf{g}|\mathcal{F}_{t-1})}}-\sum_{j=0}^{\infty}\sum_{\mathbf{g}\in\mathcal{G}_N}\frac{f_{t,j,\mathbf{g}}}{f(\boldsymbol{\epsilon}_t|\mathcal{F}_{t-1})}\frac{\theta\lambda_t\mathbf{g}^T\Sigma_{t,j,\mathbf{g}}^{-1}(\boldsymbol{\epsilon}_t-\boldsymbol{\theta}_{t,j,\mathbf{g}})}{\sqrt{\lambda_t+\theta^2\lambda_t^2E(\mathbf{g}^T\Sigma_{t,j,\mathbf{g}}^{-1}\mathbf{g}|\mathcal{F}_{t-1})}}.\end{aligned}$$

where $E(n_t|\mathcal{F}_t)$ is the ex-post expectation of the arrivals of jumps. $\mathrm{Var}(\nabla_{t,j,\mathbf{g}}^{\phi}|\mathcal{F}_{t-1})$ is calculated as follows.

$$\begin{aligned}\mathrm{Var}(\nabla_{t,j,\mathbf{g}}^{\phi}|\mathcal{F}_{t-1}) =&\mathrm{Var}(\frac{\partial\log p(n_t=j|\mathcal{F}_{t-1})}{\partial\phi_t}|\mathcal{F}_{t-1})+\mathrm{Var}(\frac{\partial\log f(\boldsymbol{\epsilon_t}|\mathcal{F}_{t-1},n_t=j,\mathbf{b}_t=\mathbf{g})}{\partial\phi_t}|\mathcal{F}_{t-1})\\ &+2\mathrm{Cov}(\frac{\partial\log p(n_t=j|\mathcal{F}_{t-1})}{\partial\phi_t}|\mathcal{F}_{t-1},\frac{\partial\log f(\boldsymbol{\epsilon_t},n_t=j,\mathbf{b}_t=\mathbf{g})}{\partial\phi_t}|\mathcal{F}_{t-1})\\ =&E((\frac{\partial\log p(n_t=j|\mathcal{F}_{t-1})}{\partial\phi_t})^2|\mathcal{F}_{t-1})+E(-\frac{\partial^2\log f(\boldsymbol{\epsilon_t}|\mathcal{F}_{t-1},n_t=j,\mathbf{b}_t=\mathbf{g})}{\partial{\phi_t}^2}|\mathcal{F}_{t-1})\\ =&\lambda_t+\theta^2\lambda_t^2E(\mathbf{g}^T\Sigma_{t,j,\mathbf{g}}^{-1}\mathbf{g}|\mathcal{F}_{t-1})\end{aligned}\tag{A.1}$$

This equation holds based on the fact that $\boldsymbol{\epsilon}_t$ truly follows $f(\boldsymbol{\epsilon_t}|\mathcal{F}_{t-1},n_t=j,\mathbf{b}_t=\mathbf{g})$ conditional on $\mathcal{F}_{t-1},n_t=j,\mathbf{b}_t=\mathbf{g}$, and n_t follows $p(n_t=j|\mathcal{F}_{t-1})$ given $\mathcal{F}_{t-1}$.

The natural extension of the method described in Ballestra et al. (2023) involves scaling $\nabla_{t,j,\mathbf{g}}^{\phi}$ by its conditional variance under $\mathcal{F}_{t-1},n_t=j,\mathbf{b}_t=\mathbf{g}$. However, we choose to condition solely on $\mathcal{F}_{t-1}$ because $\nabla_{t,j,\mathbf{g}}^{\phi}$ have no raodnmness given $\mathcal{F}_{t-1},n_t=j$ and $b_{i,t}=0$ for all $i=1,\cdots,N$.

A.2 Derivation of the Driving Force of l_t.

The driving force of l_t is calculated as

$$\begin{aligned}\tilde{s}_t^l &= \sum_{j=0}^{\infty} \sum_{\mathbf{g} \in \mathcal{G}_N} \frac{f_{t,j,\mathbf{g}}}{f(\boldsymbol{\epsilon}_t|\mathcal{F}_{t-1})} \frac{\nabla_{t,j,\mathbf{g}}^l}{\sqrt{\mathrm{Var}(\nabla_{t,j,\mathbf{g}}^l)}} \\ &= \frac{\sum_{i=1}^N E(g_i|\mathcal{F}_t) - Np_t}{\sqrt{Np_t(1-p_t)}}. \end{aligned} \tag{A.2}$$

where $E(g_i|\mathcal{F}_t)$ is the ex-post expectation of the jump indication in the asset i.

B Alternative Specification of the COMARJIS Model.

We estimate an alternative specification of the CARJIST model, wherein the driving force is scaled by the conditional variance without the square root operation. This model is estimated for the five regional banks: First Foundation Inc. (FFWM), First Republic Bank (FRCB), SVB Financial Group (SVB), Signature Bank (SBNY), and Western Alliance Bancorporation (WAL). The parameter estimates are reported in table 12. Figure 17 shows the extracted model variables. Figure 18 reports the conditional volatility. Figure 19 illustrates the ex-ante and ex-post probabilities that multiple jumps occur concurrently across more than three regional banks.

Table 12: Parameter estimates of the CARJIST model with the alternative scaling. First Foundation Inc. (FFWM), First Republic Bank (FRCB), SVB Financial Group (SVB), Signature Bank (SBNY), and Western Alliance Bancorporation (WAL) are investigated.

δ_{FFWM}	1.287 ***
δ_{FRCB}	1.971 ***
δ_{SVB}	2.461 ***
δ_{SBNY}	2.005 ***
δ_{WAL}	1.319 ***
θ	0.195 ***
$\bar{\phi}$	0.674 ***
$\bar{l}$	0.134 ***
a_ϕ	0.995 ***
b_ϕ	0.121 ***
a_l	0.858 ***
b_l	0.354 ***
$b_{\phi,l}$	0.161
$b_{l,\phi}$	0.039 ***

* Denote significance level at the 10 % level.
** Denote significance level at the 5 % level.
*** Denote significance level at the 1 % level.

(a)

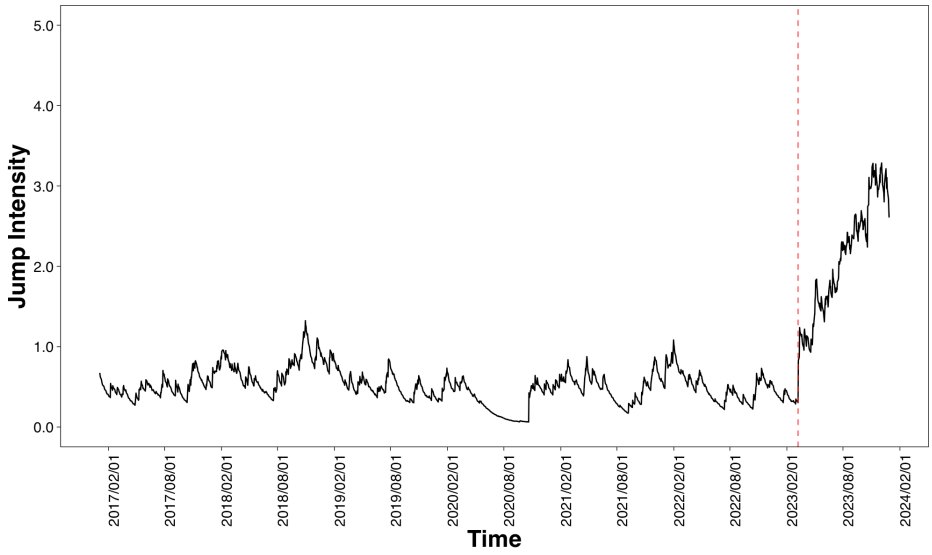

(b)

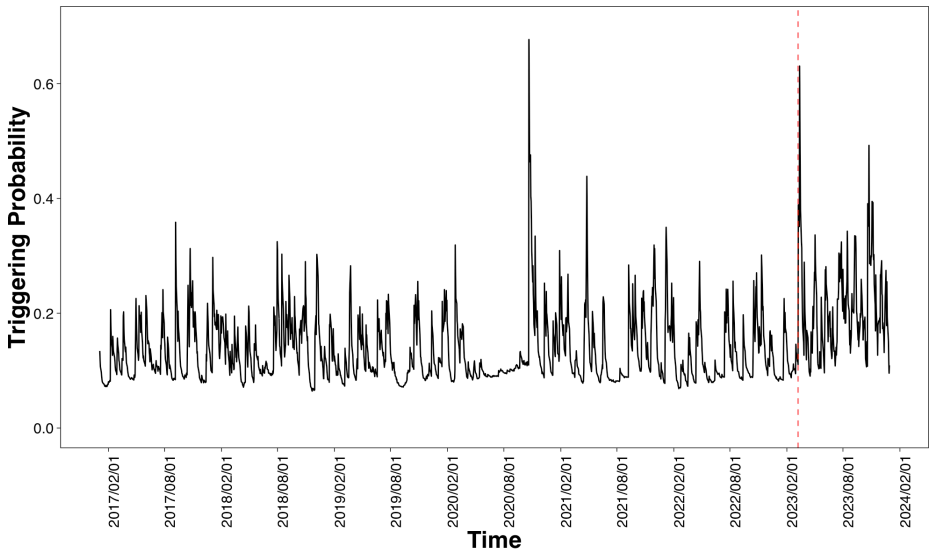

Figure 17: (a) jump intensity and (b) triggering probability of five regional banks extracted from the CARJIST model with the alternative scaling. The red point represents the value on Mar 9, 2023.

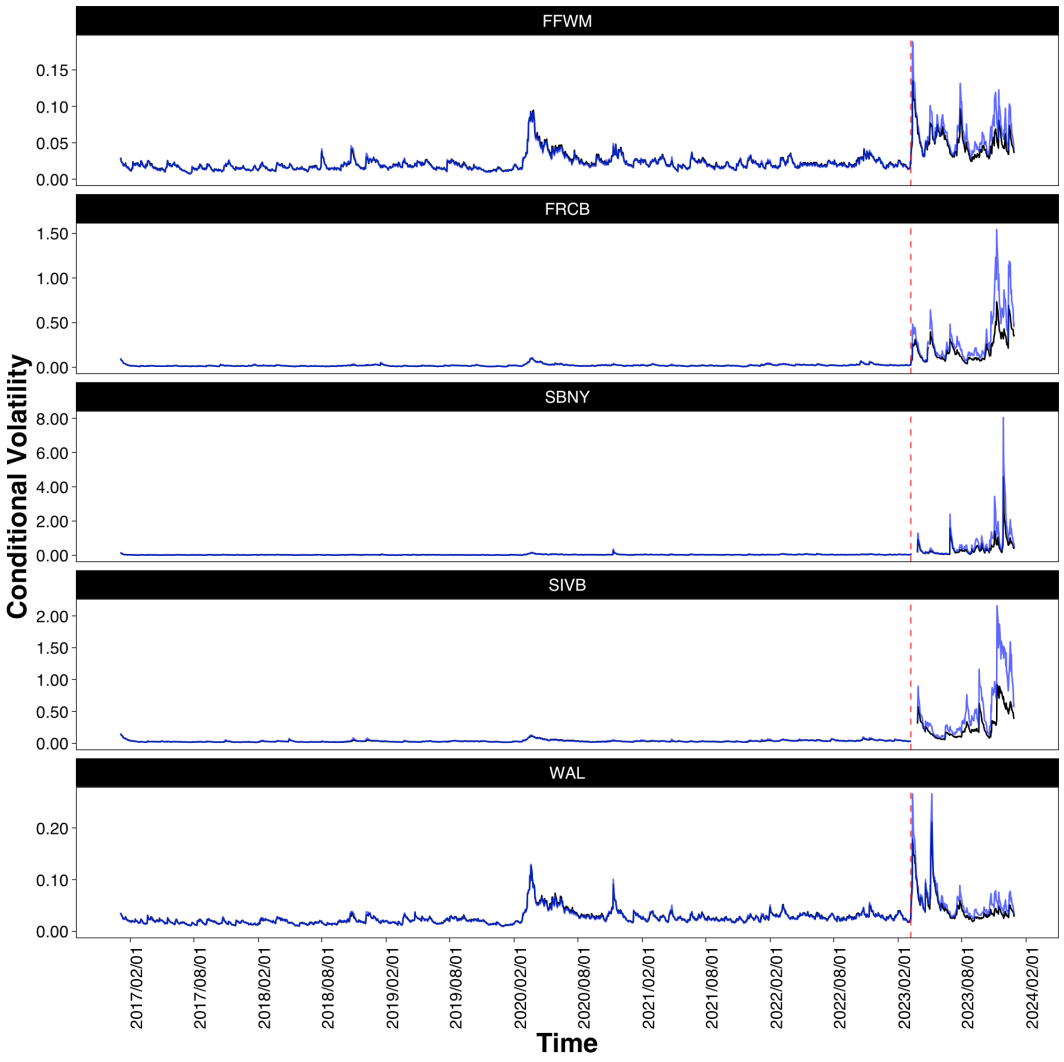

Figure 18: The time-varying conditional volatility of five regional banks from the CARJIST model with the alternative scaling. The blue line is the conditional volatility, and the black line is the EGARCH component. The red line represents Mar 9, 2023. First Foundation Inc. (FFWM), First Republic Bank (FRCB), SVB Financial Group (SVB), Signature Bank (SBNY), and Western Alliance Bancorporation (WAL) are investigated.

(a)

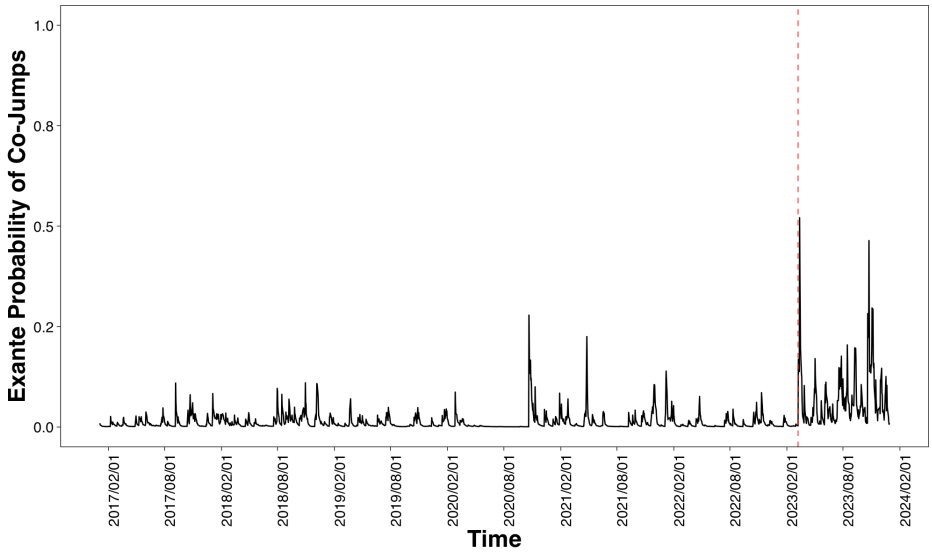

(b)

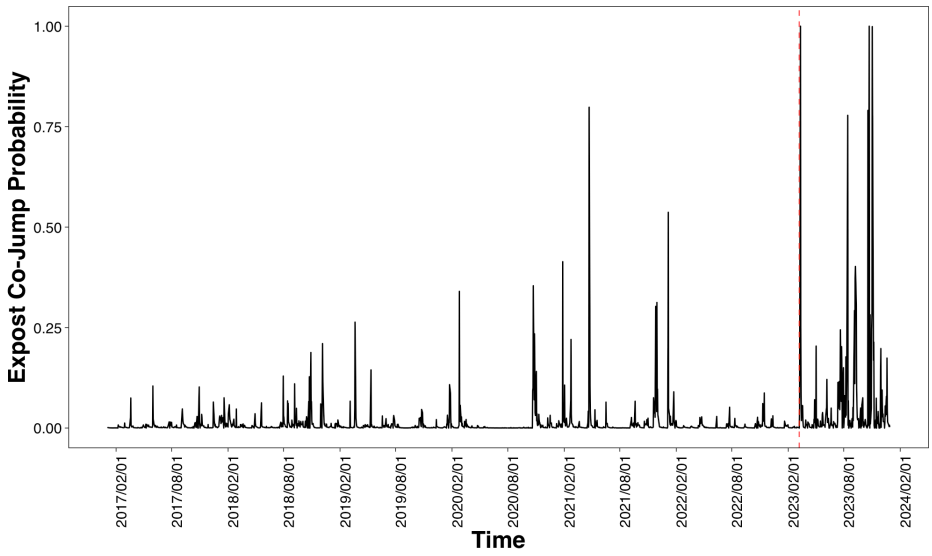

Figure 19: The (a) ex-ante and (b) ex-post probability of common jumps based on the CARJIST model with the alternative scaling. The red point represents the value on Mar 9, 2023.

C Parameter Estimates of the CARJIST Model for BAC, CITI, JPM, USB, WFC and SVB.

We report the parameter estimates of the CARJIST model for the BAC, CITI, JPM, USB, WFC and SVB. Table 13 shows the estimates for the EGARCH(1,1) parts, and table 14 shows the estimates for the rest of the parameters.

Table 13: Parameter estimates of EGARCH(1,1) model for five commercial banks and SVB. Bank of America Corporation (BAC), Citigroup Inc. (CITI), JP Morgan (JPM), U.S. Bancorp (USB), Wells Fargo & Company (WFC) and SVB Financial Group (SVB) are investigated.

	BAC	CITI	JPM	USB	WF	SVB
θ	0.0009^{***}	0.0006^{***}	0.0010^{***}	0.0006^{***}	0.0004^{***}	0.0028^{***}
α	0.95^{***}	0.97^{***}	0.97^{***}	0.96^{***}	0.97^{***}	0.99^{***}
β	0.11^{***}	0.11^{***}	0.09^{***}	0.15^{***}	0.10^{***}	0.13^{***}

* Denote significance level at the 10 % level.
** Denote significance level at the 5 % level.
*** Denote significance level at the 1 % level.

Table 14: Parameter estimates of the CARJIST model for five commercial banks and SVB. Bank of America Corporation (BAC), Citigroup Inc. (CITI), JP Morgan (JPM), U.S. Bancorp (USB), Wells Fargo & Company (WFC) and SVB Financial Group (SVB) are investigated.

δ_{BAC}	0.564^{***}
δ_{CITI}	0.960^{***}
δ_{JPM}	0.773^{***}
δ_{USB}	1.054^{***}
δ_{WF}	1.055^{***}
δ_{SVB}	2.085^{***}
θ	-0.099^{***}
$\bar{\phi}$	0.136^{*}
$\bar{l}$	-2.21^{***}
a_ϕ	0.579^{***}
b_ϕ	0.740^{***}
a_l	0.976^{***}
b_l	0.086
$b_{\phi,l}$	0.269^{***}
$b_{l,\phi}$	0.351^{***}

* Denote significance level at the 10 % level.
** Denote significance level at the 5 % level.
*** Denote significance level at the 1 % level.